

# LOGARITHMIC COEFFICIENTS AND GENERALIZED MULTIFRACTALITY OF WHOLE-PLANE SLE

BERTRAND DUPLANTIER<sup>(1)</sup>, XUAN HIEU HO<sup>(2)</sup>, THANH BINH LE<sup>(2)</sup>,  
AND MICHEL ZINSMEISTER<sup>(2)</sup>

ABSTRACT. It has been shown that for  $f$  an instance of the whole-plane SLE conformal map from the unit disk  $\mathbb{D}$  to the slit plane, the derivative moments  $\mathbb{E}(|f'(z)|^p)$  can be written in a closed form for certain values of  $p$  depending continuously on the SLE parameter  $\kappa \in (0, \infty)$ . We generalize this property to the mixed moments,  $\mathbb{E}\left(\frac{|f'(z)|^p}{|f(z)|^q}\right)$ , along integrability curves in the moment plane  $(p, q) \in \mathbb{R}^2$  depending continuously on  $\kappa$ , by extending the so-called Beliaev–Smirnov equation to this case. The generalization of this integrability property to the  $m$ -fold transform of  $f$  is also given. We define a generalized integral means spectrum,  $\beta(p, q; \kappa)$ , corresponding to the singular behavior of the mixed moments above. The average generalized spectrum of whole-plane SLE takes four possible forms, separated by five phase transition lines in the moment plane  $\mathbb{R}^2$ , whereas the average generalized spectrum of the  $m$ -fold whole-plane SLE is directly obtained from a linear map acting in that plane. We also conjecture the form of the universal generalized integral means spectrum.

## 1. INTRODUCTION

1.1. **Logarithmic coefficients.** Consider  $f$ , a holomorphic function in the unit disk  $\mathbb{D}$ ,

$$(1) \quad f(z) = \sum_{n \geq 0} a_n z^n.$$

Bieberbach observed in 1916 [4] that if  $f$  is further assumed to be injective, then

$$|a_2| \leq 2|a_1|,$$

---

*Date:* May 28, 2015.

*Key words and phrases.* Whole-plane SLE, logarithmic moments, Beliaev–Smirnov equation, generalized integral means spectrum, universal spectrum.

The first author would like to thank the Isaac Newton Institute (INI) for Mathematical Sciences, Cambridge, for its support and hospitality during the program on Random Geometry where part of this work was completed. He was partially supported by a fellowship from the Simons Foundation while at the INI. The research by the second author is supported by a joint scholarship from MENESR and Région Centre; the third author is supported by a scholarship of the Government of Vietnam.

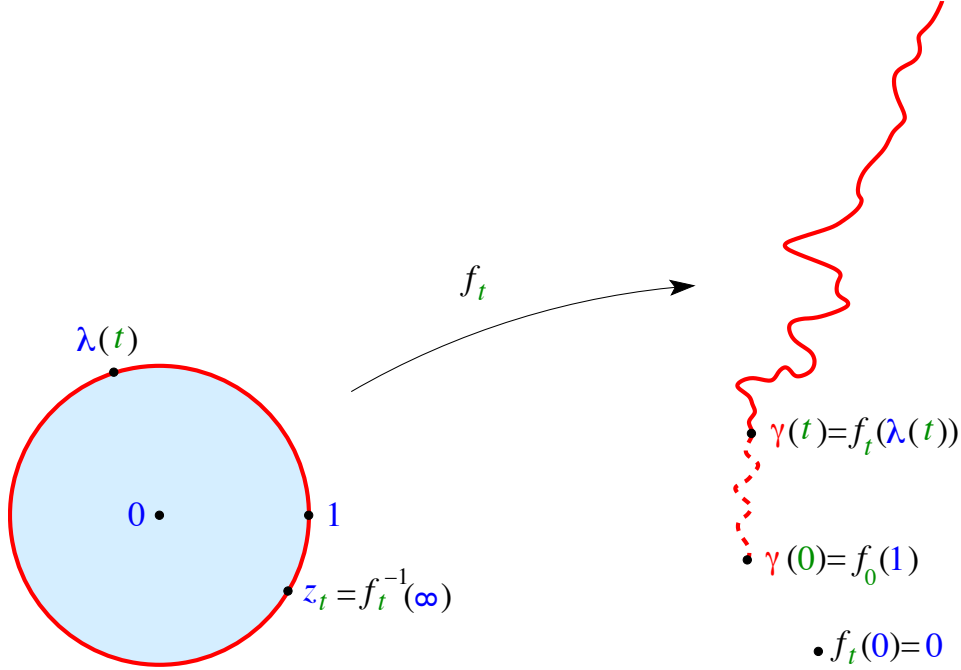


FIGURE 1. Loewner map  $z \mapsto f_t(z)$  from  $\mathbb{D}$  to the slit domain  $\Omega_t = \mathbb{C} \setminus \gamma([t, \infty))$  (here slit by a single curve  $\gamma([t, \infty))$ ) for  $\text{SLE}_{\kappa \leq 4}$ . One has  $f_t(0) = 0, \forall t \geq 0$ . At  $t = 0$ , the driving function  $\lambda(0) = 1$ , so that the image of  $z = 1$  is at the tip  $\gamma(0) = f_0(1)$  of the curve.

and he conjectured that  $|a_n| \leq n|a_1|$  for all  $n > 2$ . This famous conjecture has been proved in 1984 by de Branges [5]. A crucial ingredient of his proof is the theory of growth processes that was developed by Loewner in 1923 [22], precisely in order to solve the  $n = 3$  case of the Bieberbach conjecture.

Let  $\gamma : [0, \infty) \rightarrow \mathbb{C}$  be a simple curve such that  $|\gamma(t)| \rightarrow +\infty$  as  $t \rightarrow +\infty$  and such that  $\gamma(t) \neq 0, t \geq 0$ . Let  $\Omega_t = \mathbb{C} \setminus \gamma([t, \infty))$  and  $f_t : \mathbb{D} = \{|z| \leq 1\} \rightarrow \Omega_t$  be the Riemann map characterized by  $f_t(0) = 0, f_t'(0) > 0$  (See Fig. 1). It is easy to see that  $t \mapsto f_t'(0)$  is an increasing continuous function, diverging to  $+\infty$  as  $t \rightarrow +\infty$ . Assuming that  $f_0'(0) = 1$ , and changing parameterization if necessary, we may set  $f_t'(0) = e^t, t \geq 0$ . Loewner has shown that  $f_t$  satisfies the following PDE:

$$(2) \quad \frac{\partial}{\partial t} f_t(z) = z \frac{\partial}{\partial z} f_t(z) \frac{\lambda(t) + z}{\lambda(t) - z},$$

where  $\lambda : [0, \infty) \rightarrow \partial\mathbb{D}$  is a continuous function on the unit circle. With the sole information that  $|\lambda(t)| = 1, \forall t$ , he could prove that  $|a_3| \leq 3|a_1|$ .

Besides Loewner's theory of growth processes, de Branges' proof also heavily relied on the consideration, developed by Grunsky [12] and later Lebedev and

Milin [17], of *logarithmic* coefficients. More precisely, if  $f : \mathbb{D} \rightarrow \mathbb{C}$  is holomorphic and injective with  $f(0) = 0$ , we may consider the power series,

$$(3) \quad \log \frac{f(z)}{z} = 2 \sum_{n \geq 1} \gamma_n z^n.$$

The purpose of introducing this logarithm was to prove Robertson's conjecture [26], which was known to imply Bieberbach's. Let  $f$  be in the class  $\mathcal{S}$  of schlicht functions, i.e., holomorphic and injective in the unit disk, and normalized as  $f(0) = 0$ ,  $f'(0) = 1$ . There is a branch  $f^{[2]}$  of  $z \mapsto \sqrt{f(z^2)}$  which is an odd function in  $\mathcal{S}$ . Let us then write

$$(4) \quad f^{[2]}(z) := z \sqrt{f(z^2)/z^2} = \sum_{n=0}^{\infty} b_{2n+1} z^{2n+1},$$

with  $b_1 = 1$ . Robertson's conjecture states that:

$$(5) \quad \forall n \geq 0, \sum_{k=0}^n |b_{2k+1}|^2 \leq n + 1.$$

The Lebedev and Milin approach to this conjecture consisted in observing that

$$\log \frac{f^{[2]}(\sqrt{z})}{\sqrt{z}} = \frac{1}{2} \log \frac{f(z)}{z},$$

and consequently that

$$\sum_{n=0}^{\infty} b_{2n+1} z^n = \exp \left( \sum_{n=1}^{\infty} \gamma_n z^n \right).$$

They proved what is now called the second Lebedev-Milin inequality, a combinatorial inequality connecting the coefficients of any power series to those of its exponential, namely

$$(6) \quad \forall n \geq 0, \sum_{k=0}^n |b_{2k+1}|^2 \leq (n+1) \exp \left( \frac{1}{n+1} \sum_{m=1}^n \sum_{k=1}^m \left( k |\gamma_k|^2 - \frac{1}{k} \right) \right).$$

This naturally led Milin [24] to conjecture that

$$(7) \quad \forall f \in \mathcal{S}, \forall n \geq 1, \sum_{m=1}^n \sum_{k=1}^m \left( k |\gamma_k|^2 - \frac{1}{k} \right) \leq 0;$$

this conjecture, that de Branges proved in 1984, implies Robertson's, hence Bieberbach's conjecture.

Returning to Loewner's theory, his derivation of Eq. (2) above is only half of the story. There is indeed a converse: given any continuous function  $\lambda : [0, +\infty[ \rightarrow \mathbb{C}$  with  $|\lambda(t)| = 1$  for  $t \geq 0$ , the the Loewner equation (2), supplemented by the boundary ("initial") condition,  $\lim_{t \rightarrow +\infty} f_t(e^{-t}z) = z$ , has a solution  $(t, z) \mapsto$

$f_t(z)$ , such that  $(f_t(z))_{t \geq 0}$  is a chain of Riemann maps onto simply connected domains  $(\Omega_t)$  that are increasing with  $t$ .

In 1999, Schramm [28] introduced into the Loewner equation the *random* driving function,

$$(8) \quad \lambda(t) := \sqrt{\kappa} B_t,$$

where  $B_t$  is standard one dimensional Brownian motion and  $\kappa$  a non-negative parameter, thereby making Eq. (2) a stochastic PDE, and creating the celebrated *Schramm-Loewner Evolution*  $\text{SLE}_\kappa$ .

The associated conformal maps  $f_t$  from  $\mathbb{D}$  to  $\mathbb{C} \setminus \gamma([t, \infty))$ , obeying (2) for (8), define the *interior whole-plane* Schramm-Loewner evolution. Their coefficients  $a_n(t)$ , which are random variables, are defined by a normalized series expansion, as described in the following proposition [9].

**Proposition 1.1.** *Let  $(f_t(z))_{t \geq 0}$ ,  $z \in \mathbb{D}$ , be the interior Schramm-Loewner whole-plane process driven by  $\lambda(t) = e^{i\sqrt{\kappa} B_t}$  in Eq. (2). We write*

$$(9) \quad f_t(z) = e^t \left( z + \sum_{n \geq 2} a_n(t) z^n \right).$$

and for its logarithm,

$$(10) \quad \log \frac{e^{-t} f_t(z)}{z} = 2 \sum_{n \geq 1} \gamma_n(t) z^n.$$

Then the conjugate whole-plane Schramm-Loewner evolution  $e^{-i\sqrt{\kappa} B_t} f_t(e^{i\sqrt{\kappa} B_t} z)$  has the same law as  $f_0(z)$ , hence  $e^{i(n-1)\sqrt{\kappa} B_t} a_n(t) \stackrel{(\text{law})}{=} a_n(0)$ . From this and Eqs. (9), (10), follows the identity  $e^{in\sqrt{\kappa} B_t} \gamma_n(t) \stackrel{(\text{law})}{=} \gamma_n(0)$ . In the sequel, we set:  $a_n := a_n(0)$  and  $\gamma_n := \gamma_n(0)$ .

The starting point of the present article is the observation, made in Ref. [8], that the  $\text{SLE}_\kappa$  process, in its *interior* whole-plane version, has a rich algebraic structure, giving rise to a host of (integrability-like) closed form results. The first hint was the fact that, beyond the coefficient expectations  $\mathbb{E}(a_n)$  for Eq. (9), the coefficient squared moments,  $\mathbb{E}(|a_n|^2)$ , have very simple expressions for specific values of  $\kappa$ . This has been developed in detail in Refs. [9] and [18] (see also [19, 20, 21]), by using the so-called Beliaev-Smirnov equation, a PDE obeyed by the derivative moments  $\mathbb{E}(|f'(z)|^p)$ , originally derived by the latter authors [3] to study the average integral means spectrum of the (interior version of the) whole-plane  $\text{SLE}_\kappa$  map. Note also that similar ideas already appeared in Ref. [13], where A. Kemppainen studied in detail the coefficients associated with the Schramm-Loewner evolution, using a stationarity property of SLE [14]. However, the focus there was on expectations of the moments of those coefficients, rather than on the moments of their moduli.

Here, we study the logarithmic coefficients (10) of whole-plane  $\text{SLE}_\kappa$  and the generalizations thereof, which are obtained by introducing *generalized moments* for the whole-plane SLE map,  $\mathbb{E}(|f'(z)|^p/|f(z)|^q)$ , for  $(p, q) \in \mathbb{R}^2$ . The manifold identities so obtained in the  $(p, q)$ -plane encompass all previous results.

**1.2. Main results.** A first motivation of this article is the proof, originally obtained for small  $n$  by the third author [16], of the following.

**Theorem 1.1.** *Let  $f(z) := f_0(z)$  be the time 0 unbounded whole-plane  $\text{SLE}_\kappa$  map, in the same setting as in Proposition 1.1, such that*

$$\log \frac{f(z)}{z} = 2 \sum_{n \geq 1} \gamma_n z^n;$$

then, for  $\kappa = 2$ ,

$$\mathbb{E}(|\gamma_n|^2) = \frac{1}{2n^2}, \quad \forall n \geq 1.$$

The idea behind the proof of Theorem 1.1 is to differentiate (3),

$$\frac{d}{dz} \log \frac{f(z)}{z} = \frac{f'(z)}{f(z)} - \frac{1}{z},$$

and to compute  $\mathbb{E}\left(\left|\frac{f'(z)}{f(z)}\right|^2\right)$ . We indeed prove:

**Theorem 1.2.** *Let  $f$  be the interior whole-plane  $\text{SLE}_\kappa$  map, in the same setting as in Theorem 1.1; then for  $\kappa = 2$ ,*

$$\mathbb{E}\left(\left|z \frac{f'(z)}{f(z)}\right|^2\right) = \frac{(1-z)(1-\bar{z})}{1-z\bar{z}}.$$

Let us briefly return to the Lebedev-Milin theory. By Theorem 1.1, we have for  $\text{SLE}_2$ ,

$$\mathbb{E}\left(\sum_{m=1}^n \sum_{k=1}^m \left(k|\gamma_k|^2 - \frac{1}{k}\right)\right) = -\frac{1}{2} \sum_{m=1}^n \sum_{k=1}^m \frac{1}{k} = -\frac{n+1}{2} \sum_{k=2}^{n+1} \frac{1}{k},$$

which gives an example of the validity ‘‘in expectation’’ of the Milin conjecture. Recalling Definition (4), we also get, in expectation, a check of Robertson’s conjecture (5):

$$\mathbb{E}\left(\log \frac{\sum_{k=0}^n |b_{2k+1}|^2}{n+1}\right) \leq -\frac{1}{2} \sum_{k=2}^{n+1} \frac{1}{k}.$$

Theorem 1.2 is actually a consequence of Theorems 3.1 and 4.2 of Sections 3 and 4 below, which give expressions in closed form for the mixed moments,

$$(11) \quad (a) \quad \mathbb{E}\left(\frac{(f'(z))^{p/2}}{(f(z))^{q/2}}\right); \quad (b) \quad \mathbb{E}\left(\frac{|f'(z)|^p}{|f(z)|^q}\right),$$

along an integrability curve  $\mathcal{R}$ , which is a *parabola* in the  $(p, q)$  plane depending on the SLE parameter  $\kappa$ . In fact, we establish a general integrability result along the parabola  $\mathcal{R}$  for the SLE *two-point function*:

$$G(z_1, \bar{z}_2) := \mathbb{E} \left( z_1^{\frac{q}{2}} \frac{(f'(z_1))^{\frac{p}{2}}}{(f(z_1))^{\frac{q}{2}}} \overline{\left[ z_2^{\frac{q}{2}} \frac{(f'(z_2))^{\frac{p}{2}}}{(f(z_2))^{\frac{q}{2}}} \right]} \right).$$

The mixed moments (11) can also be seen respectively as the value  $G(z, 0)$  of this SLE two-point function at  $(z_1 = z, z_2 \rightarrow 0)$  for (a), and the value  $G(z, \bar{z})$  at coinciding points,  $z_1 = z_2 = z$ , for (b). These integrability theorems, which provide full generalizations of the results of Refs. [9] and [18], give rise to a host of new algebraic identities concerning the (interior) whole-plane  $\text{SLE}_\kappa$  random map.

These integrability results can be generalized to the so-called  $m$ -fold symmetric transforms  $f^{[m]}$ ,  $m \in \mathbb{N} \setminus \{0\}$ , of the whole-plane SLE map  $f$ . Interestingly enough, a linear map in the  $(p, q)$ -moment plane allows one to directly relate the mixed moments of the  $m$ -fold map to those of  $f$ . The extension of the definition to  $m \in \mathbb{Z} \setminus \{0\}$  exchanges exterior and interior whole-plane SLE maps, and relates their mixed moments; in particular, the case considered by Beliaev and Smirnov in Ref. [3] appears as the  $m = -1$  transform of the interior SLE map studied here and in Ref. [9]. We thus believe that the general approach proposed here to consider generalized mixed moments in the  $(p, q)$ -plane is the natural one for dealing with the properties of whole-plane SLE: in particular, it directly relates the inner and outer versions in a unified framework.

Because of the introduction in Eq. (11) of the mixed moments (b) of moduli of  $f'$  and  $f$  for whole-plane SLE, it is also natural to define a *generalized integral means spectrum*  $\beta(p, q)$ , depending on  $p$  and  $q$ . It is associated with the possible singular behavior of circle integrals of such moments in  $\mathbb{D}$ :

$$\int_{r\partial\mathbb{D}} \mathbb{E} \left( \frac{|f'(z)|^p}{|f(z)|^q} \right) |dz| \stackrel{(r \rightarrow 1^-)}{\asymp} (1-r)^{-\beta(p,q)},$$

in the sense of the equivalence of the logarithms of both terms.

In this article, we thus study the generalized spectrum,  $\beta(p, q; \kappa)$ , of whole-plane  $\text{SLE}_\kappa$  in the whole parameter space  $(p, q) \in \mathbb{R}^2$ . We show that it takes four possible forms,  $\beta_0(p)$ ,  $\beta_{\text{tip}}(p)$ ,  $\beta_{\text{lin}}(p)$  and  $\beta_1(p, q)$ . The first three spectra are independent of  $q$ , and are respectively given by the bulk, the tip and the linear SLE spectra appearing in the work by Beliaev and Smirnov [3] (and for the bulk case, corresponding to the harmonic measure multifractal spectrum derived earlier by the first author in Ref. [6]). The fourth spectrum,  $\beta_1(p, q)$ , is the extension to non-vanishing  $q$  of a novel integral means spectrum, which was discovered and studied in Refs. [9] and [18, 20], and which is due to the unboundedness of whole-plane SLE. As shown in Ref. [9], this spectrum is also closely related to the SLE tip exponents obtained by quantum gravity techniques in Ref. [7], and to the so-called radial SLE derivative exponents of Ref. [15]. Five different

phase transition lines then appear to partition the  $(p, q)$ -plane in four different domains, whose precise form is given.

The generalization of this four-domain structure to the generalized integral means spectrum of  $m$ -fold transforms,  $f^{[m]}$ ,  $m \in \mathbb{Z} \setminus \{0\}$ , is obtained in a straightforward way from the above mentioned linear map in  $(p, q)$  co-ordinates. This structure appears so robust that the *universal* generalized spectrum  $B(p, q)$ , i.e., the maximum of  $\beta(p, q)$  over all unbounded univalent functions in the unit disk, presents a similar partition of the mixed moment plane. We give a precise conjecture for its four forms, which incorporates known results on the standard universal spectra for univalent, unbounded, functions [11, 25].

**1.3. Synopsis.** This article is organized as follows. Section 2 deals with logarithmic coefficients and with the proof of Theorems 1.1 and 1.2. It sets up the martingale techniques needed for dealing with mixed moments. Section 3 uses them for the study of the complex one-point function  $(a)$  in (11), which is shown to obey a simple differential equation in complex variable  $z$ . This leads to Theorem 3.1, which establishes a closed form for this function along the integrability parabola  $\mathcal{R}$  in the  $(p, q)$ -plane. Section 4 is concerned with the moduli one-point function  $(b)$  in (11), and more generally, with the SLE two-point function  $G(z_1, \bar{z}_2)$ . A PDE in  $(z_1, \bar{z}_2)$  is derived for  $G(z_1, \bar{z}_2)$ , which yields a proof of Theorem 4.2 establishing closed form expressions for  $G$  for all  $(p, q) \in \mathcal{R}$ . Section 5 deals with the generalization of the previous integrability results to the  $m$ -fold symmetric transforms  $f^{[m]}$ ,  $m \in \mathbb{Z} \setminus \{0\}$ , of the whole-plane SLE map  $f$ . Section 6 is devoted to the study of the averaged generalized spectrum  $\beta(p, q; \kappa)$  of the whole-plane  $\text{SLE}_\kappa$  random map  $f$ , as well as to the averaged generalized integral means spectrum  $\beta^{[m]}(p, q; \kappa)$  of the  $m$ -fold transform  $f^{[m]}$  for  $m \in \mathbb{Z} \setminus \{0\}$ . Of particular interest are the five phase transition lines separating the four different analytic expressions of  $\beta$  (or  $\beta^{[m]}$ ) in the moment plane. A more geometric derivation of these transition lines, based on a conic representation of the spectra, is given in Section 7. In the final Section 8, we give a full description of the expected form for the universal generalized integral means spectrum,  $B(p, q)$ , in terms of known or conjectured results on the standard universal spectrum for univalent functions.

**Acknowledgments.** It is a pleasure to thank Kari Astala for extended discussions about the universal generalized integral means spectrum.

## 2. EXPECTATIONS OF LOGARITHMIC COEFFICIENTS

**2.1. A martingale computation.** In this section, we first prove the following:

**Theorem 2.1.** *Let  $f(z)$  be the whole-plane  $\text{SLE}_\kappa$  map, in the same setting as in Theorem 1.1; then for  $\kappa = 2$ ,*

$$\mathbb{E}(\gamma_n) = \begin{cases} -1/2, & n = 1, \\ 0, & n \geq 2. \end{cases}$$

Differentiating both sides of (3), we get

$$(12) \quad z \frac{f'(z)}{f(z)} = 1 + 2 \sum_{n \geq 1} n \gamma_n z^n.$$

Let us now consider

$$(13) \quad G(z) := \mathbb{E} \left( z \frac{f'(z)}{f(z)} \right),$$

and, following Ref [3], aim at finding a partial differential equation satisfied by  $G$ . For the benefit of the reader not familiar with Ref. [3], let us detail the strategy of that paper that we will apply in various contexts here.

The starting point is to consider the radial SLE $_{\kappa}$ , solution to the ODE

$$\partial_t g_t(z) = g_t(z) \frac{\lambda(t) + g_t(z)}{\lambda(t) - g_t(z)}, \quad z \in \mathbb{D},$$

with the initial condition  $g_0(z) = z$ , and where  $\lambda(t) = e^{i\sqrt{\kappa}B_t}$ . The map  $g_t$  conformally maps a subdomain of the unit disk onto the latter. As we shall see shortly, the whole-plane map  $f$  is rather related to the map  $g_t^{-1}$ , but this last function satisfies, by Loewner's theory, a PDE not well-suited to Itô calculus. To overcome this difficulty, one runs backward the ODE of radial SLE, i.e., one compares  $g_t^{-1}$  to  $g_{-t}$ . This is the purpose of Lemma 1 in [3] (an analog of Lemma 3.1 in Ref. [27]), which states that, for  $t \in \mathbb{R}$ ,  $g_{-t}(z)$  has the same law as the process  $\tilde{f}_t(z)$ , defined as follows.

**Definition 2.2.** The (conjugate, inverse) radial SLE process  $\tilde{f}_t$  is defined, for  $t \in \mathbb{R}$ , as

$$(14) \quad \tilde{f}_t(z) := g_t^{-1}(z\lambda(t))/\lambda(t).$$

The lemma then results from the simple observation that

$$\tilde{f}_s(z) = \hat{g}_{-s}(z),$$

where, for fixed  $s \in \mathbb{R}$ , the new process  $\hat{g}_t(z) := g_{s+t} \circ g_s^{-1}(z\lambda(s))/\lambda(s)$  can be shown to be a radial SLE. This lemma implies in particular that  $\tilde{f}_t$  is solution to the ODE:

$$(15) \quad \partial_t \tilde{f}_t(z) = \tilde{f}_t(z) \frac{\tilde{f}_t(z) + \lambda(t)}{\tilde{f}_t(z) - \lambda(t)}, \quad \tilde{f}_0(z) = z.$$

To apply Itô's stochastic calculus, one then uses Lemma 2 in Ref. [3], which is a version of the SLE's Markov property,

$$\tilde{f}_t(z) = \lambda(s) \tilde{f}_{t-s}(\tilde{f}_s(z)/\lambda(s)).$$

To finish, one has to relate the whole-plane SLE to the (modified) radial one. This is done through Lemma 3 in [3], which is in our present setting (with a change of an  $e^{-t}$  convergence factor there to an  $e^t$  factor here, when passing from the exterior to the interior of the unit disk  $\mathbb{D}$ ):



**Lemma 2.3.** *The limit in law,  $\lim_{t \rightarrow +\infty} e^t \tilde{f}_t(z)$ , exists, and has the same law as the (time zero) interior whole-plane random map  $f_0(z)$ :*

$$\lim_{t \rightarrow +\infty} e^t \tilde{f}_t(z) \stackrel{(\text{law})}{=} f_0(z).$$

Let us now turn to the proof of Theorem 2.1.

*Proof.* Let us introduce the auxiliary, time-dependent, radial variant of the SLE one-point function  $G(z)$  (13) above,

$$(16) \quad \tilde{G}(z, t) := \mathbb{E} \left( z \frac{\tilde{f}'_t(z)}{\tilde{f}_t(z)} \right),$$

where  $\tilde{f}_t$  is a modified radial SLE map at time  $t$  as in Definition 2.2. Owing to Lemma (2.3), we have

$$(17) \quad \lim_{t \rightarrow +\infty} \tilde{G}(z, t) = G(z).$$

We then use a martingale technique to obtain an equation satisfied by  $\tilde{G}(z, t)$ . For  $s \leq t$ , define  $\mathcal{M}_s := \mathbb{E} \left( \frac{\tilde{f}'_t(z)}{\tilde{f}_t(z)} | \mathcal{F}_s \right)$ , where  $\mathcal{F}_s$  is the  $\sigma$ -algebra generated by  $\{B_u, u \leq s\}$ .  $(\mathcal{M}_s)_{s \geq 0}$  is by construction a martingale. Because of the Markov property of SLE, we have [3]

$$\begin{aligned} \mathcal{M}_s &= \mathbb{E} \left( \frac{\tilde{f}'_t(z)}{\tilde{f}_t(z)} | \mathcal{F}_s \right) = \mathbb{E} \left( \frac{\tilde{f}'_s(z) \tilde{f}'_{t-s}(\tilde{f}_s(z)/\lambda(s))}{\lambda(s) \tilde{f}_{t-s}(\tilde{f}_s(z)/\lambda(s))} | \mathcal{F}_s \right) \\ &= \frac{\tilde{f}'_s(z)}{\lambda(s)} \mathbb{E} \left( \frac{\tilde{f}'_{t-s}(\tilde{f}_s(z)/\lambda(s))}{\tilde{f}_{t-s}(\tilde{f}_s(z)/\lambda(s))} | \mathcal{F}_s \right) \\ &= \frac{\tilde{f}'_s(z)}{\tilde{f}_s(z)} \tilde{G}(z_s, \tau), \end{aligned}$$

where  $z_s := \tilde{f}_s(z)/\lambda(s)$ , and  $\tau := t - s$ .

We have from Eq. (15)

$$(18) \quad \begin{aligned} \partial_s \log \tilde{f}'_s &= \frac{\partial_z \left[ \tilde{f}'_s \frac{\tilde{f}_s + \lambda(s)}{\tilde{f}_s - \lambda(s)} \right]}{\tilde{f}'_s} = \frac{\tilde{f}_s + \lambda(s)}{\tilde{f}_s - \lambda(s)} - \frac{2\lambda(s)\tilde{f}_s}{(\tilde{f}_s - \lambda(s))^2} \\ &= 1 - \frac{2}{(1 - z_s)^2}, \end{aligned}$$

$$(19) \quad \partial_s \log \tilde{f}_s = \frac{\partial_s \tilde{f}_s}{\tilde{f}_s} = \frac{z_s + 1}{z_s - 1},$$

$$(20) \quad dz_s = z_s \left[ \frac{z_s + 1}{z_s - 1} - \frac{\kappa}{2} \right] ds - iz_s \sqrt{\kappa} dB_s.$$

The coefficient of the  $ds$ -drift term of the Itô derivative of  $\mathcal{M}_s$  is obtained from the above as,

$$(21) \quad \frac{\tilde{f}'_s(z)}{\tilde{f}_s(z)} \left[ -\frac{2z_s}{(1-z_s)^2} + z_s \left( \frac{z_s+1}{z_s-1} - \frac{\kappa}{2} \right) \partial_z - \partial_\tau - \frac{\kappa}{2} z_s^2 \partial_z^2 \right] \tilde{G}(z_s, \tau),$$

and vanishes by the (local) martingale property. Because  $\tilde{f}_s$  is univalent,  $\tilde{f}'_s$  does not vanish in  $\mathbb{D}$ , therefore the bracket above vanishes.

Owing to the existence of the limit (17), we can now take the  $\tau \rightarrow +\infty$  limit in the above, and obtain the ODE,

$$(22) \quad \begin{aligned} \mathcal{P}(\partial)[G(z)] &:= -\frac{2z}{(1-z)^2} G(z) + z \left( \frac{z+1}{z-1} - \frac{\kappa}{2} \right) G'(z) - \frac{\kappa}{2} z^2 G''(z) \\ &= \left[ -\frac{2z}{(1-z)^2} + z \left( \frac{z+1}{z-1} \right) \partial_z - \frac{\kappa}{2} (z\partial_z)^2 \right] G(z) = 0. \end{aligned}$$

Following Ref. [9], we now look for solutions to Eq. (22) of the form  $\varphi_\alpha(z) := (1-z)^\alpha$ . We have

$$\mathcal{P}(\partial)[\varphi_\alpha] = A(2, 2, \alpha)\varphi_\alpha + B(2, \alpha)\varphi_{\alpha-1} + C(2, \alpha)\varphi_{\alpha-2},$$

where, in anticipation of the notation that will be introduced in Section 3 below,

$$\begin{aligned} A(2, 2, \alpha) &:= \alpha - \frac{\kappa}{2}\alpha^2, \\ B(2, \alpha) &:= 2 - \left( 3 + \frac{\kappa}{2} \right) \alpha + \kappa\alpha^2, \\ C(2, \alpha) &:= -2 + \left( 2 + \frac{\kappa}{2} \right) \alpha - \frac{\kappa}{2}\alpha^2, \end{aligned}$$

with, identically,  $A + B + C = 0$ . The linear independence of  $\varphi_\alpha, \varphi_{\alpha-1}, \varphi_{\alpha-2}$  thus shows that  $\mathcal{P}(\partial)[\varphi_\alpha] = 0$  is equivalent to  $A = B = C = 0$ , which yields  $\kappa = 2, \alpha = 1$ , and  $G(z) = 1 - z$ . From Definition (13), we thus get

**Lemma 2.4.** *Let  $f(z) = f_0(z)$  be the interior whole-plane SLE<sub>2</sub> map at time 0, in the same setting as in Proposition 1.1; we then have*

$$\mathbb{E} \left( z \frac{f'(z)}{f(z)} \right) = 1 - z.$$

Theorem 2.1 follows from Lemma 2.4 and the series expansion (12). □

**2.2. Proof of Theorem 1.1.** Using (12), we get

$$(23) \quad \left| z \frac{f'(z)}{f(z)} \right|^2 = 1 + 2 \sum_{n \geq 1} n \gamma_n (z^n + \bar{z}^n) + \sum_{n \geq 1} \sum_{m \geq 1} nm \gamma_n \bar{\gamma}_m z^n \bar{z}^m.$$

On the other hand, by Theorem 1.2,

$$\mathbb{E} \left( \left| z \frac{f'(z)}{f(z)} \right|^2 \right) = \frac{(1-z)(1-\bar{z})}{(1-z\bar{z})} = 1 - \sum_{n \geq 0} z^{n+1} \bar{z}^n - \sum_{n \geq 0} z^n \bar{z}^{n+1} + 2 \sum_{n \geq 1} z^n \bar{z}^n.$$

Identifying the latter with the expectation of (23), we get the expected coefficients

$$\begin{aligned} \mathbb{E}(\gamma_1) &= -1/2, \quad \mathbb{E}(\gamma_n) = 0, \quad n \geq 2, \\ \mathbb{E}(|\gamma_n|^2) &= \frac{1}{2n^2}, \quad n \geq 1, \\ \mathbb{E}(\gamma_n \bar{\gamma}_{n+1}) &= -\frac{1}{n(n+1)}, \quad \mathbb{E}(\gamma_n \bar{\gamma}_{n+k}) = 0, \quad n \geq 1, k \geq 2, \end{aligned}$$

which encompasses Theorems 1.1 and 2.1.

### 3. SLE ONE-POINT FUNCTION

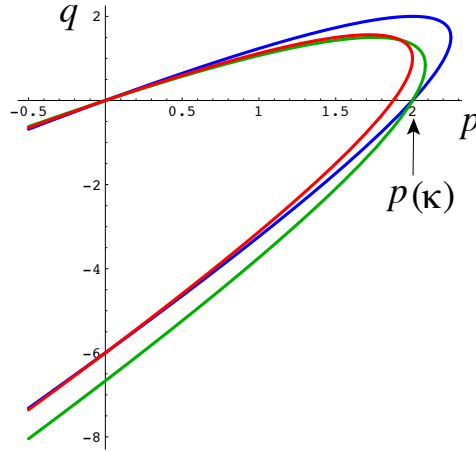


FIGURE 2. Integral curves  $\mathcal{R}$  of Theorem 3.1, for  $\kappa = 2$  (blue),  $\kappa = 4$  (red), and  $\kappa = 6$  (green). In addition to the origin, the  $q = 0$  intersection point with the  $p$ -axis is at  $p(\kappa) := (6 + \kappa)(2 + \kappa)/8\kappa$ , with  $p(2) = p(6) = 2$  [9, 18].

Let us now turn to the natural generalization of Lemma 2.4.

**Theorem 3.1.** *Let  $f(z) = f_0(z)$  be the interior whole-plane  $SLE_\kappa$  map at time zero, in the same setting as in Proposition 1.1. Consider the curve  $\mathcal{R}$ , defined parametrically by*

$$(24) \quad p = -\frac{\kappa}{2}\gamma^2 + \left(2 + \frac{\kappa}{2}\right)\gamma, \quad 2p - q = \left(1 + \frac{\kappa}{2}\right)\gamma, \quad \gamma \in \mathbb{R}.$$

On  $\mathcal{R}$ , the whole-plane  $SLE_\kappa$  one-point function has the integrable form,

$$\mathbb{E}\left(\frac{(f'(z))^{\frac{p}{2}}}{(f(z)/z)^{\frac{q}{2}}}\right) = (1 - z)^\gamma.$$

*Remark 3.2.* Eq. (24) describes a parabola in the  $(p, q)$  plane (see (Fig. 2), which is given in Cartesian coordinates by

$$(25) \quad 2\kappa \left( \frac{2p - q}{2 + \kappa} \right)^2 - (4 + \kappa) \frac{2p - q}{2 + \kappa} + p = 0,$$

with two branches,

$$(26) \quad \begin{aligned} \gamma &= \gamma_0^\pm(p) := \frac{1}{2\kappa} \left( 4 + \kappa \pm \sqrt{(4 + \kappa)^2 - 8\kappa p} \right), \quad p \leq \frac{(4 + \kappa)^2}{8\kappa}, \\ q &= 2p - \left( 1 + \frac{\kappa}{2} \right) \gamma_0^\pm(p). \end{aligned}$$

or, equivalently,

$$(27) \quad 2p = q + \frac{2 + \kappa}{8\kappa} \left( 6 + \kappa \pm \sqrt{(6 + \kappa)^2 - 16\kappa q} \right), \quad q \leq \frac{(6 + \kappa)^2}{16\kappa}.$$

*Proof.* Our aim is to derive an ODE satisfied by the whole-plane SLE one-point function,

$$(28) \quad G(z) := \mathbb{E} \left( z^{\frac{q}{2}} \frac{(f'(z))^{\frac{p}{2}}}{(f(z))^{\frac{q}{2}}} \right),$$

which, by construction, stays finite at the origin and such that  $G(0) = 1$ .

Let us introduce the shorthand notation,

$$(29) \quad X_t(z) := \frac{(\tilde{f}'_t(z))^{\frac{p}{2}}}{(\tilde{f}_t(z))^{\frac{q}{2}}},$$

where  $\tilde{f}_t$  is the conjugate, reversed radial SLE process in  $\mathbb{D}$ , as introduced in Definition 2.2, and such that by Lemma 2.3, the limit,  $\lim_{t \rightarrow +\infty} e^t \tilde{f}_t(z) \stackrel{(\text{law})}{=} f_0(z)$ , is the same in law as the whole-plane map at time zero. Applying the same method as in the previous section, we consider the time-dependent function

$$(30) \quad \tilde{G}(z, t) := \mathbb{E} \left( z^{\frac{q}{2}} X_t(z) \right),$$

such that

$$(31) \quad \lim_{t \rightarrow +\infty} \exp \left( \frac{p - q}{2} t \right) \tilde{G}(z, t) = G(z).$$

Consider now the martingale  $(\mathcal{M}_s)_{t \geq s \geq 0}$ , defined by

$$\mathcal{M}_s = \mathbb{E}(X_t(z) | \mathcal{F}_s).$$

By the SLE Markov property we get, setting  $z_s := \tilde{f}_s(z)/\lambda(s)$ ,

$$(32) \quad \mathcal{M}_s = X_s(z) \tilde{G}(z_s, \tau), \quad \tau := t - s.$$

As before, the partial differential equation satisfied by  $\tilde{G}(z_s, \tau)$  is obtained by expressing the fact that the  $ds$ -drift term of the Itô differential of Eq. (32),

$$d\mathcal{M}_s = \tilde{G} dX_s + X_s d\tilde{G},$$

vanishes. The differential of  $X_s$  is simply computed from Eqs. (18) and (19) above as:

$$(33) \quad dX_s(z) = X_s(z)F(z)ds,$$

$$F(z) := \frac{p}{2} \left[ 1 - \frac{2}{(1-z)^2} \right] - \frac{q}{2} \left[ 1 - \frac{2}{1-z} \right].$$

The Itô differential  $d\tilde{G}$  brings in the  $ds$  terms proportional to  $\partial_{z_s}\tilde{G}$ ,  $\partial_{z_s}^2\tilde{G}$ , and  $\partial_\tau\tilde{G}$ ; therefore, in the PDE satisfied by  $\tilde{G}$ , the latter terms are exactly the same as in the PDE (21). We therefore directly arrive at the vanishing condition of the overall drift term coefficient in  $d\mathcal{M}_s$ ,

$$(34) \quad X_s(z) \left[ F(z_s) + z_s \left( \frac{z_s+1}{z_s-1} - \frac{\kappa}{2} \right) \partial_z - \partial_\tau - \frac{\kappa}{2} z_s^2 \partial_z^2 \right] \tilde{G}(z_s, \tau) = 0.$$

Since  $X_s(z)$  does not vanish in  $\mathbb{D}$ , the bracket in (34) must identically vanish:

$$(35) \quad \left[ F(z_s) + z_s \frac{z_s+1}{z_s-1} \partial_z - \partial_\tau - \frac{\kappa}{2} (z_s \partial_z)^2 \right] \tilde{G}(z_s, \tau) = 0,$$

where we used  $z\partial_z + z^2\partial_z^2 = (z\partial_z)^2$ .

To derive the ODE satisfied by  $G(z)$  (28), we first recall its expression as the limit (30), which further implies

$$\lim_{\tau \rightarrow +\infty} \exp\left(\frac{p-q}{2}\tau\right) \partial_\tau \tilde{G}(z, \tau) = -\frac{p-q}{2} G(z).$$

Multiplying the PDE (34) satisfied by  $\tilde{G}$  by  $\exp(\frac{p-q}{2}\tau)$  and letting  $\tau \rightarrow +\infty$ , we get

$$(36) \quad \mathcal{P}(\partial)[G(z)] := \left[ -\frac{\kappa}{2} (z\partial_z)^2 - \frac{1+z}{1-z} z\partial_z + F(z) + \frac{p-q}{2} \right] G(z)$$

$$= \left[ -\frac{\kappa}{2} (z\partial_z)^2 - \frac{1+z}{1-z} z\partial_z - \frac{p}{(1-z)^2} + \frac{q}{1-z} + p - q \right] G(z) = 0.$$

We now look specifically for solutions to (36), together with the boundary condition  $G(0) = 1$ , of the form  $\varphi_\alpha(z) = (1-z)^\alpha$ . This function satisfies the simple differential operator algebra [9]

$$(37) \quad \mathcal{P}(\partial)[\varphi_\alpha] = A(p, q, \alpha)\varphi_\alpha + B(q, \alpha)\varphi_{\alpha-1} + C(p, \alpha)\varphi_{\alpha-2},$$

where

$$(38) \quad A(p, q, \alpha) := p - q + \alpha - \frac{\kappa}{2}\alpha^2,$$

$$(39) \quad B(q, \alpha) := q - \left( 3 + \frac{\kappa}{2} \right) \alpha + \kappa\alpha^2,$$

$$(40) \quad C(p, \alpha) := -p + \left( 2 + \frac{\kappa}{2} \right) \alpha - \frac{\kappa}{2}\alpha^2,$$

such that, identically,  $A + B + C = 0$ . Because  $\varphi_\alpha, \varphi_{\varphi-1}, \varphi_{\alpha-2}$  are linearly independent, the condition  $\mathcal{P}(\partial)[\varphi_\gamma]$  is equivalent to the system  $A = C = 0$ , hence  $C(p, \gamma) = 0$  and  $A(p, q, \gamma) - C(p, \gamma) = 2p - q - (1 + \kappa/2)\gamma = 0$ . It yields precisely the parabola parametrization (24) given in Theorem 3.1, and has for solution (26).  $\square$

#### 4. SLE TWO-POINT FUNCTION

**4.1. Beliaev–Smirnov type equations.** In this section, we will determine the mixed moments of moduli,  $\mathbb{E}\left(\frac{|f'(z)|^p}{|f(z)|^q}\right)$ , for  $(p, q)$  belonging to the same parabola  $\mathcal{R}$  as in Theorem 3.1, and where  $f = f_0$  is the (time zero) interior whole-plane  $\text{SLE}_\kappa$  map.

In contradistinction to the method used in Refs. [3, 9] for writing a PDE obeyed by  $\mathbb{E}(|f'(z)|^p)$ , we shall use here a slightly different approach, building on the results obtained in Section 2.1. We shall study the SLE two-point function for  $z_1, z_2 \in \mathbb{D}$ ,

$$(41) \quad G(z_1, \bar{z}_2) := \mathbb{E}\left(z_1^{\frac{q}{2}} \frac{(f'(z_1))^{\frac{p}{2}}}{(f(z_1))^{\frac{q}{2}}} \overline{\left[ z_2^{\frac{q}{2}} \frac{(f'(z_2))^{\frac{p}{2}}}{(f(z_2))^{\frac{q}{2}}} \right]}\right).$$

As before, we define a time-dependent, auxiliary two-point function,

$$(42) \quad \begin{aligned} \tilde{G}(z_1, \bar{z}_2, t) &:= \mathbb{E}\left(z_1^{\frac{q}{2}} \frac{(\tilde{f}'_t(z_1))^{\frac{p}{2}}}{(\tilde{f}_t(z_1))^{\frac{q}{2}}} \overline{\left[ z_2^{\frac{q}{2}} \frac{(\tilde{f}'_t(z_2))^{\frac{p}{2}}}{(\tilde{f}_t(z_2))^{\frac{q}{2}}} \right]}\right) \\ &= \mathbb{E}\left(z_1^{\frac{q}{2}} X_t(z_1) \overline{z_2^{\frac{q}{2}} X_t(z_2)}\right), \end{aligned}$$

where as above  $\tilde{f}_t$  is the reverse radial  $\text{SLE}_\kappa$  process 2.2, and where we used the shorthand notation (29). This time, the two-point function (41) is the limit

$$(43) \quad \lim_{t \rightarrow +\infty} e^{(p-q)t} \tilde{G}(z_1, \bar{z}_2, t) = G(z_1, \bar{z}_2).$$

Let us define the two-point martingale  $(\mathcal{M}_s)_{t \geq s \geq 0}$ , with

$$\mathcal{M}_s := \mathbb{E}(X_t(z_1) \overline{X_t(z_2)} | \mathcal{F}_s).$$

By the Markov property of SLE,

$$(44) \quad \mathbb{E}(X_t(z_1) \overline{X_t(z_2)} | \mathcal{F}_s) = X_s(z_1) \overline{X_s(z_2)} \tilde{G}(z_{1s}, \bar{z}_{2s}, \tau), \quad \tau := t - s,$$

where

$$(45) \quad z_{1s} := \tilde{f}_s(z_1)/\lambda(s); \quad \bar{z}_{2s} := \overline{\tilde{f}_s(z_2)/\lambda(s)} = \overline{\tilde{f}_s(z_2)}\lambda(s).$$

Their Itô differentials,  $dz_{1s}$  and  $d\bar{z}_{2s}$ , are as in (20),

$$(46) \quad \begin{aligned} dz_{1s} &= z_{1s} \left[ \frac{z_{1s} + 1}{z_{1s} - 1} - \frac{\kappa}{2} \right] ds - i\sqrt{\kappa} z_{1s} dB_s, \\ d\bar{z}_{2s} &= \bar{z}_{2s} \left[ \frac{\bar{z}_{2s} + 1}{\bar{z}_{2s} - 1} - \frac{\kappa}{2} \right] ds + i\sqrt{\kappa} \bar{z}_{2s} dB_s. \end{aligned}$$

As before, the partial differential equation satisfied by  $\tilde{G}(z_{1s}, z_{2s}, \tau)$  is obtained by expressing the fact that the  $ds$ -drift term of the Itô differential of Eq. (44),

$$(47) \quad d\mathcal{M}_s = [dX_s(z_1)\overline{X_s(z_2)} + X_s(z_1)d\overline{X_s(z_2)}] \tilde{G} + X_s(z_1)\overline{X_s(z_2)} d\tilde{G},$$

vanishes.

The differentials of  $X_s, \overline{X_s}$  are as in Eq. (33) above:

$$(48) \quad \begin{aligned} dX_s(z_1) &= X_s(z_1)F(z_{1s})ds, \quad d\overline{X_s(z_2)} = \overline{X_s(z_2)}F(\bar{z}_{2s})ds, \\ F(z) &:= \frac{p}{2} - \frac{q}{2} - \frac{p}{(1-z)^2} + \frac{q}{1-z}. \end{aligned}$$

We thus obtain the simple expression

$$(49) \quad d\mathcal{M}_s = X_s(z_1)\overline{X_s(z_2)} \left[ [F(z_{1s}) + F(\bar{z}_{2s})] \tilde{G} ds + d\tilde{G} \right],$$

and the vanishing of the  $ds$ -drift term in  $d\mathcal{M}_s$  requires that of the drift term in the right-hand side bracket in (49), since  $X_s(z)$  does not vanish in  $\mathbb{D}$ .

The Itô differential of  $\tilde{G}(z_{1s}, \bar{z}_{2s}, \tau)$  can be obtained from Eqs. (46) and Itô calculus as

$$(50) \quad \begin{aligned} d\tilde{G}(z_{1s}, \bar{z}_{2s}, \tau) &= \partial_1 \tilde{G} dz_{1s} + \bar{\partial}_2 \tilde{G} d\bar{z}_{2s} - \partial_\tau \tilde{G} ds \\ &\quad - \frac{\kappa}{2} z_{1s}^2 \partial_1^2 \tilde{G} ds - \frac{\kappa}{2} \bar{z}_{2s}^2 \bar{\partial}_2^2 \tilde{G} ds + \kappa z_{1s} \bar{z}_{2s} \partial_1 \bar{\partial}_2 \tilde{G} ds, \end{aligned}$$

where use was made of the shorthand notations,  $\partial_1 := \partial_{z_1}$  and  $\bar{\partial}_2 := \partial_{\bar{z}_2}$ . We observe that the only coupling between the  $z_{1s}, \bar{z}_{2s}$  variables arises in the last term of (50), the other terms simply resulting from the independent contributions of the  $z_{1s}$  and  $\bar{z}_{2s}$  parts.

Using again the Itô differentials (46), we can rewrite (50) as

$$(51) \quad \begin{aligned} d\tilde{G} &= -i\sqrt{\kappa} (z_{1s}\partial_1 - \bar{z}_{2s}\bar{\partial}_2) \tilde{G} dB_s \\ &\quad + \frac{z_{1s} + 1}{z_{1s} - 1} z_{1s} \partial_1 \tilde{G} ds + \frac{\bar{z}_{2s} + 1}{\bar{z}_{2s} - 1} \bar{z}_{2s} \bar{\partial}_2 \tilde{G} ds - \partial_\tau \tilde{G} ds \\ &\quad - \frac{\kappa}{2} (z_{1s}\partial_1 - \bar{z}_{2s}\bar{\partial}_2)^2 \tilde{G} ds, \end{aligned}$$

where we used the obvious formal identity

$$(52) \quad (z_1\partial_1)^2 + (\bar{z}_2\bar{\partial}_2)^2 - 2z_1\partial_1\bar{z}_2\bar{\partial}_2 = (z_1\partial_1 - \bar{z}_2\bar{\partial}_2)^2.$$

At this stage, comparing the computations (49) and (51) above with those in the one-point martingale study in Section 2.1, it is clear that the PDE obeyed by

$\tilde{G} = \tilde{G}(z_{1s}, \bar{z}_{2s}, \tau)$  is obtained as two duplicates of Eq. (35), completed as in (52) by the derivative coupling between variables  $z_{1s}, \bar{z}_{2s}$ :

$$(53) \quad \left[ F(z_{1s}) + z_{1s} \frac{z_{1s} + 1}{z_{1s} - 1} \partial_1 + F(\bar{z}_{2s}) + \bar{z}_{2s} \frac{\bar{z}_{2s} + 1}{\bar{z}_{2s} - 1} \bar{\partial}_2 - \partial_\tau - \frac{\kappa}{2} (z_{1s} \partial_1 - \bar{z}_{2s} \bar{\partial}_2)^2 \right] \tilde{G} = 0.$$

The existence of the limit (43) further implies that of

$$\lim_{\tau \rightarrow \infty} e^{(p-q)\tau} \partial_\tau \tilde{G}(z_1, \bar{z}_2, \tau) = -(p-q)G(z_1, \bar{z}_2).$$

Multiplying the PDE (53) satisfied by  $\tilde{G}$  by  $\exp((p-q)\tau)$  and letting  $\tau \rightarrow +\infty$ , then gives the expected PDE for  $G(z_1, \bar{z}_2)$ . It can be most compactly written in terms of the ODE (36) as

$$(54) \quad [\mathcal{P}(\partial_1) + \mathcal{P}(\bar{\partial}_2) + \kappa z_1 \partial_1 \bar{z}_2 \bar{\partial}_2] G(z_1, \bar{z}_2) = 0,$$

and its fully explicit expression is

$$(55) \quad \begin{aligned} \mathcal{P}(D)[G(z_1, \bar{z}_2)] &= -\frac{\kappa}{2} (z_1 \partial_1 - \bar{z}_2 \bar{\partial}_2)^2 G - \frac{1+z_1}{1-z_1} z_1 \partial_1 G - \frac{1+\bar{z}_2}{1-\bar{z}_2} \bar{z}_2 \bar{\partial}_2 G \\ &+ \left[ -\frac{p}{(1-z_1)^2} - \frac{p}{(1-\bar{z}_2)^2} + \frac{q}{1-z_1} + \frac{q}{1-\bar{z}_2} + 2p - 2q \right] G = 0. \end{aligned}$$

**4.2. Moduli one-point function.** Note that one can take the  $z_1 = z_2 = z$  case in Definition (41) above, thereby obtaining the moduli one-point function,

$$(56) \quad G(z, \bar{z}) = \mathbb{E} \left( |z|^q \frac{|f'(z)|^p}{|f(z)|^q} \right).$$

Because of Eq. (55), it obeys the corresponding ODE,

$$(57) \quad \begin{aligned} \mathcal{P}(D)[G(z, \bar{z})] &= -\frac{\kappa}{2} (z \partial - \bar{z} \bar{\partial})^2 G - \frac{1+z}{1-z} z \partial G - \frac{1+\bar{z}}{1-\bar{z}} \bar{z} \bar{\partial} G \\ &+ \left[ -\frac{p}{(1-z)^2} - \frac{p}{(1-\bar{z})^2} + \frac{q}{1-z} + \frac{q}{1-\bar{z}} + 2p - 2q \right] G = 0, \end{aligned}$$

which is the generalization to  $q \neq 0$  of the Beliaev–Smirnov equation studied in Refs. [9] and [18].

### 4.3. Integrable case.

**Lemma 4.1.** *The space of formal series  $F(z_1, \bar{z}_2) = \sum_{k, \ell \in \mathbb{N}} a_{k, \ell} z_1^k \bar{z}_2^\ell$ , with complex coefficients and that are solutions of the PDE (55), is one-dimensional.*

*Proof.* We assume that  $F$  is a solution to (55) with  $F(0, 0) = 0$ ; it suffices to prove that, necessarily,  $F = 0$ . We argue by contradiction: If not, consider the minimal (necessarily non constant) term  $a_{k, \ell} z_1^k \bar{z}_2^\ell$  in the series of  $F$ , with  $a_{k, \ell} \neq 0$  and  $k + \ell$  minimal (and non vanishing). Then  $\mathcal{P}(D)[F]$  (55) will have a minimal term, equal to  $-a_{k, \ell} \left[ \frac{\kappa}{2} (k - \ell)^2 + k + \ell \right] z_1^k \bar{z}_2^\ell$ , which is non-zero, contradicting the fact that  $\mathcal{P}(D)[F]$  vanishes.  $\square$



As a second step, following Ref. [9], let us consider the action of the operator  $\mathcal{P}(D)$  of (55) on a function of the factorized form  $\varphi(z_1)\varphi(\bar{z}_2)P(z_1, \bar{z}_2)$ , which we write, in a shorthand notation, as  $\varphi\bar{\varphi}P$ . By Leibniz's rule, it is given by

$$\begin{aligned} \mathcal{P}(D)[\varphi\bar{\varphi}P] &= -\frac{\kappa}{2}\varphi\bar{\varphi}(z_1\partial_1 - \bar{z}_2\bar{\partial}_2)^2P - \kappa(z_1\partial_1 - \bar{z}_2\bar{\partial}_2)(\varphi\bar{\varphi})(z_1\partial_1 - \bar{z}_2\bar{\partial}_2)P \\ &\quad + \kappa(z_1\partial_1\varphi)(\bar{z}_2\bar{\partial}_2\bar{\varphi})P - \varphi\bar{\varphi}\frac{1+z_1}{1-z_1}z_1\partial_1P - \varphi\bar{\varphi}\frac{1+\bar{z}_2}{1-\bar{z}_2}\bar{z}_2\bar{\partial}_2P \\ &\quad - \left[ \frac{\kappa}{2}\bar{\varphi}(z_1\partial_1)^2\varphi + \frac{\kappa}{2}\varphi(\bar{z}_2\bar{\partial}_2)^2\bar{\varphi} + \bar{\varphi}\frac{1+z_1}{1-z_1}z_1\partial_1\varphi + \varphi\frac{1+\bar{z}_2}{1-\bar{z}_2}\bar{z}_2\bar{\partial}_2\bar{\varphi} \right] P \\ &\quad + \left[ -\frac{p}{(1-z_1)^2} - \frac{p}{(1-\bar{z}_2)^2} + \frac{q}{1-z_1} + \frac{q}{1-\bar{z}_2} + 2p - 2q \right] \varphi\bar{\varphi}P. \end{aligned}$$

Note that the operator  $z_1\partial_1 - \bar{z}_2\bar{\partial}_2$  is antisymmetric with respect to  $z_1, \bar{z}_2$ ; therefore, if we choose a symmetric function,  $P(z_1, \bar{z}_2) = P(z_1\bar{z}_2)$ , the first line of  $\mathcal{P}(D)[\varphi\bar{\varphi}P]$  above identically vanishes.

One then looks for solutions to (55) of the particular form,

$$G(z_1, \bar{z}_2) = \varphi_\alpha(z_1)\varphi_\alpha(\bar{z}_2)P(z_1\bar{z}_2),$$

where, as before,  $\varphi_\alpha(z) = (1-z)^\alpha$ . The action of the differential operator then takes the simple form,

$$\begin{aligned} \mathcal{P}(D)[\varphi_\alpha\bar{\varphi}_\alpha P] &= z_1\bar{z}_2\varphi_{\alpha-1}\bar{\varphi}_{\alpha-1}(\kappa\alpha^2P - 2(1-z_1\bar{z}_2)P') \\ &\quad + \mathcal{P}(\partial_1)[\varphi_\alpha]\bar{\varphi}_\alpha P + \mathcal{P}(\partial_2)[\bar{\varphi}_\alpha]\varphi_\alpha P, \end{aligned}$$

where  $P'$  is the derivative of  $P$  with respect to  $z_1\bar{z}_2$ , and  $\mathcal{P}(\partial)$  is the so-called boundary operator (36) [9].

The ODE,  $\kappa\alpha^2P(x) - 2(1-x)P'(x) = 0$  with  $x = z_1\bar{z}_2$  and  $P(0) = 1$ , has for solution  $P(z_1\bar{z}_2) = (1-z_1\bar{z}_2)^{-\kappa\alpha^2/2}$ . It is then sufficient to pick for  $\alpha$  the value  $\gamma = \gamma_0^\pm(p)$  (26) such that  $\mathcal{P}(\partial)[\varphi_\gamma] = 0$ , as obtained in the proof of Theorem 3.1, to get a solution of the PDE,  $\mathcal{P}(D)[\varphi_\gamma\bar{\varphi}_\gamma P] = 0$  (55). By uniqueness of the solution with  $G(0, 0) = 1$ , it gives the explicit form of the SLE two-point function,

$$G(z_1, \bar{z}_2) = \varphi_\gamma(z_1)\varphi_\gamma(\bar{z}_2)(1-z_1\bar{z}_2)^{-\kappa\gamma^2/2}.$$

We thus get:

**Theorem 4.2.** *Let  $f(z) = f_0(z)$  be the interior whole-plane  $\text{SLE}_\kappa$  map in the setting of Proposition (1.1); then, for  $(p, q)$  belonging to the parabola  $\mathcal{R}$  defined in Theorem 3.1 by Eqs. (24) or (25) or (26), and for any pair  $(z_1, z_2) \in \mathbb{D} \times \mathbb{D}$ ,*

$$\mathbb{E} \left( z_1^{\frac{q}{2}} \frac{(f'(z_1))^{\frac{p}{2}}}{(f(z_1))^{\frac{q}{2}}} \overline{z_2^{\frac{q}{2}} \frac{(f'(z_2))^{\frac{p}{2}}}{(f(z_2))^{\frac{q}{2}}}} \right) = \frac{(1-z_1)^\gamma(1-\bar{z}_2)^\gamma}{(1-z_1\bar{z}_2)^\beta}, \quad \beta = \frac{\kappa}{2}\gamma^2.$$

**Corollary 4.3.** *In the same setting as in Theorem 4.2, we have for  $z \in \mathbb{D}$ ,*

$$\mathbb{E} \left( |z|^q \frac{|f'(z)|^p}{|f(z)|^q} \right) = \frac{(1-z)^\gamma(1-\bar{z})^\gamma}{(1-z\bar{z})^\beta}, \quad \beta = \frac{\kappa}{2}\gamma^2,$$

for

$$\begin{aligned}\gamma &= \gamma_0^\pm(p) := \frac{1}{2\kappa} \left( 4 + \kappa \pm \sqrt{(4 + \kappa)^2 - 8\kappa p} \right), \quad p \leq \frac{(4 + \kappa)^2}{8\kappa}, \\ q &= 2p - \left( 1 + \frac{\kappa}{2} \right) \gamma_0^\pm(p).\end{aligned}$$

Let us stress some particular cases of interest. First, the  $p = 0$  case gives some integral means of  $f$ .

**Corollary 4.4.** *The interior whole-plane  $\text{SLE}_\kappa$  map has the integrable moments*

$$\begin{aligned}\mathbb{E} \left( \left[ \frac{f(z_1)}{z_1} \right]^{\frac{(2+\kappa)(4+\kappa)}{4\kappa}} \left[ \frac{f(z_2)}{\bar{z}_2} \right]^{\frac{(2+\kappa)(4+\kappa)}{4\kappa}} \right) &= \frac{(1 - z_1)^{\frac{4+\kappa}{\kappa}} (1 - \bar{z}_2)^{\frac{4+\kappa}{\kappa}}}{(1 - z_1 \bar{z}_2)^{\frac{(4+\kappa)^2}{2\kappa}}}, \\ \mathbb{E} \left( \left| \frac{f(z)}{z} \right|^{\frac{(2+\kappa)(4+\kappa)}{2\kappa}} \right) &= \frac{(1 - z)^{\frac{4+\kappa}{\kappa}} (1 - \bar{z})^{\frac{4+\kappa}{\kappa}}}{(1 - z\bar{z})^{\frac{(4+\kappa)^2}{2\kappa}}}.\end{aligned}$$

Second, taking  $p = q$  yields the logarithmic integral means we started with:

**Corollary 4.5.** *The interior whole-plane  $\text{SLE}_\kappa$  map  $f(z) = f_0(z)$  has the integrable logarithmic moment*

$$\begin{aligned}\mathbb{E} \left( \left[ z_1 \frac{f'(z_1)}{f(z_1)} \right]^{\frac{2+\kappa}{2\kappa}} \left[ \bar{z}_2 \frac{f'(z_2)}{f(z_2)} \right]^{\frac{2+\kappa}{2\kappa}} \right) &= \frac{(1 - z_1)^{\frac{2}{\kappa}} (1 - \bar{z}_2)^{\frac{2}{\kappa}}}{(1 - z_1 \bar{z}_2)^{\frac{2}{\kappa}}}, \\ \mathbb{E} \left( \left| z \frac{f'(z)}{f(z)} \right|^{\frac{2+\kappa}{\kappa}} \right) &= \frac{(1 - z)^{\frac{2}{\kappa}} (1 - \bar{z})^{\frac{2}{\kappa}}}{(1 - z\bar{z})^{\frac{2}{\kappa}}}.\end{aligned}$$

Theorem 1.2 describes the  $\kappa = 2$  case of the latter result.

## 5. GENERALIZATION TO PROCESSES WITH $m$ -FOLD SYMMETRY

The results of Section 4 may be generalized to functions with  $m$ -fold symmetry, with  $m$  a positive integer, as was studied in [9]. For  $f$  in class  $\mathcal{S}$ ,  $f^{[m]}(z)$  is defined as being the holomorphic branch of  $f(z^m)^{1/m}$  whose derivative is equal to 1 at 0. These are the functions in  $\mathcal{S}$  whose Taylor series is of the form  $f(z) = \sum_{k \geq 0} a_{mk+1} z^{mk+1}$ . The  $m = 2$  case corresponds to odd functions that play a crucial role in the theory of univalent functions.

One can also extend this definition to negative integers  $m$ , by considering then the  $m$ -fold transform of the outer whole-plane SLE as the conjugate by the inversion  $z \mapsto 1/z$  of the  $(-m)$ -fold transform of the inner whole-plane SLE:  $f^{[m]}(z) = 1/f^{[-m]}(1/z)$  for  $m \in \mathbb{Z} \setminus \mathbb{N}$  and  $z \in \mathbb{C} \setminus \bar{\mathbb{D}}$ . The  $m = -1$  case is of special interest:  $f^{[-1]}$  maps the exterior of the unit disk onto the inverted image of  $f(\mathbb{D})$ , which is a domain with bounded boundary. Actually, for  $f(z)$  the interior

whole-plane  $\text{SLE}_\kappa$  map considered in Ref. [9] and here,  $f^{[-1]}(z^{-1})$  is precisely the exterior whole-plane  $\text{SLE}_\kappa$  map introduced in Ref. [3].

The moments,  $\mathbb{E}(|(f^{[m]})'(z)|^p)$  (for  $m \in \mathbb{N} \setminus \{0\}$ ), as well as their associated integral means spectra were studied in Ref. [9]. Using Itô calculus, a PDE satisfied by these moments was derived for each value of  $m$ . The introduction of mixed  $(p, q)$  moments allows us to circumvent these calculations in a unified approach. To see this, notice that

$$(f^{[m]})'(z) = z^{m-1} f'(z^m) f(z^m)^{\frac{1}{m}-1}.$$

As a consequence,

$$\frac{|z|^q |(f^{[m]})'(z)|^p}{|f^{[m]}(z)|^q} = |z|^{q+p(m-1)} \frac{|f'(z^m)|^p}{|f(z^m)|^{p+\frac{q-p}{m}}},$$

so that we identically have

$$(58) \quad \mathbb{E} \left( |z|^q \frac{|(f^{[m]})'(z)|^p}{|f^{[m]}(z)|^q} \right) = G(z^m; p, q_m),$$

$$(59) \quad q_m = q_m(p, q) := p + \frac{q-p}{m},$$

with the notation,

$$(60) \quad G(z; p, q) := G(z, \bar{z}) = \mathbb{E} \left( |z|^q \frac{|f'(z)|^p}{|f(z)|^q} \right),$$

where we have made explicit the dependence on the  $(p, q)$  parameters of the SLE moduli one-point function (56) introduced in Section 3. From Theorem 4.2, we immediately get the following.

**Theorem 5.1.** *Let  $f^{[m]}$  be the  $m$ -fold whole-plane  $\text{SLE}_\kappa$  map,  $m \in \mathbb{Z} \setminus \{0\}$ , with  $z \in \mathbb{D}$  for  $m > 0$  and  $z \in \mathbb{C} \setminus \bar{\mathbb{D}}$  for  $m < 0$ . Then,*

$$\mathbb{E} \left( |z|^q \frac{|(f^{[m]})'(z)|^p}{|f^{[m]}(z)|^q} \right) = \frac{(1 - z^m)^\alpha (1 - \bar{z}^m)^\alpha}{(1 - (z\bar{z})^m)^{\frac{\kappa}{2}\alpha^2}},$$

for  $(p, q)$  belonging to the  $m$ -dependent parabola  $\mathcal{R}^{[m]}$ , given in parametric form by

$$(61) \quad p = \left(2 + \frac{\kappa}{2}\right) \alpha - \frac{\kappa}{2} \alpha^2, \quad q = \left(m + 2 + \frac{\kappa}{2}\right) \alpha - \frac{\kappa}{2} (m+1) \alpha^2, \quad \alpha \in \mathbb{R}.$$

In Cartesian coordinates, an equivalent statement is

$$\alpha = \frac{(m+1)p - q}{m \left(1 + \frac{\kappa}{2}\right)},$$

with

$$q = (m+1)p - m \frac{2+\kappa}{4\kappa} \left(4 + \kappa \pm \sqrt{(4+\kappa)^2 - 8\kappa p}\right), \quad p \leq \frac{(4+\kappa)^2}{8\kappa},$$

or,

$$p = \frac{q}{m+1} + \frac{m}{(m+1)^2} \frac{2+\kappa}{4\kappa} \left( 2m+4+\kappa \pm \sqrt{(2m+4+\kappa)^2 - 8(m+1)\kappa q} \right),$$

$$q \leq \frac{(2m+4+\kappa)^2}{8(m+1)\kappa}.$$

As for logarithmic coefficients, first observe that trivially,

$$(62) \quad \log \frac{f^{[m]}(z)}{z} = \frac{1}{m} \log \frac{f(z^m)}{z^m}.$$

From this, and Theorem 1.1, we thus get

**Corollary 5.2.** *Let  $f^{[m]}(z)$  be the  $m$ -fold whole-plane SLE $_2$  map and*

$$(63) \quad \log \frac{f^{[m]}(z)}{z} = 2 \sum_{n \geq 1} \gamma_n^{[m]} z^n;$$

then

$$\mathbb{E}(|\gamma_n^{[m]}|^2) = \begin{cases} \frac{1}{2n^2} & n = mk, \quad k \geq 1 \\ 0 & \text{otherwise.} \end{cases}$$

We can also see this result as a corollary of Theorem 5.1, which, for the logarithmic case  $p = q$ , and for any value of  $m$ , yields  $p = q = 2$  for  $\kappa = 2$  as the only integrable case.

## 6. INTEGRAL MEANS SPECTRUM

**6.1. Introduction.** In this section we aim at generalizing to the setting of the present work the integral means spectrum analysis of Refs. [3] and [9] (see also [18, 19, 20]) concerning the whole-plane SLE. The original work by Beliaev–Smirnov [3] dealt with the exterior version, whereas Ref. [9] and this work concern the interior case. We thus look for the singular behavior of the integral,

$$(64) \quad \int_{r\partial\mathbb{D}} \mathbb{E} \left( \frac{|f'(z)|^p}{|f(z)|^q} \right) |dz|,$$

for  $r \rightarrow 1^-$ , where  $f$  stands for the interior whole-plane SLE map (at time zero). The integral means spectrum  $\beta(p, q)$  corresponding to this generalized moment integral is the exponent such that

$$(65) \quad \int_{r\partial\mathbb{D}} \mathbb{E} \left( \frac{|f'(z)|^p}{|f(z)|^q} \right) |dz| \stackrel{(r \rightarrow 1^-)}{\asymp} (1-r)^{-\beta(p, q)},$$

in the sense of the equivalence of the logarithms of both terms.

As mentioned in Section 5, it is interesting to remark that the map  $\hat{f} := f^{[-1]}$ ,

$$\zeta \in \mathbb{C} \setminus \overline{\mathbb{D}} \mapsto f^{[-1]}(\zeta) := 1/f(1/\zeta),$$

is just the *exterior* whole-plane map from  $\mathbb{C} \setminus \overline{\mathbb{D}}$  to the slit plane considered by Beliaev and Smirnov in Ref. [3]. We identically have for  $0 < r < 1$ :

$$(66) \quad \int_{r^{-1}\partial\mathbb{D}} \mathbb{E} \left( |\hat{f}'(\zeta)|^p \right) |d\zeta| = r^{2p-2} \int_{r\partial\mathbb{D}} \mathbb{E} \left( \frac{|f'(z)|^p}{|f(z)|^{2p}} \right) |dz|.$$

We thus see that the standard integral mean of order  $(p, q = 0)$  for the exterior whole-plane map studied in Ref. [3] *coincides* (up to an irrelevant power of  $r$ ) with the  $(p, q)$  integral mean (64) for  $q = 2p$ , for the interior whole-plane map.

*Remark 6.1. Exterior-Interior Duality.* More generally, we obviously have

$$(67) \quad \int_{r^{-1}\partial\mathbb{D}} \mathbb{E} \left( \frac{|\hat{f}'(\zeta)|^p}{|\hat{f}(\zeta)|^{q'}} \right) |d\zeta| = r^{2p-2} \int_{r\partial\mathbb{D}} \mathbb{E} \left( \frac{|f'(z)|^p}{|f(z)|^{2p-q'}} \right) |dz|,$$

so that the  $(p, q')$  exterior integral means spectrum coincides with the  $(p, q)$  interior integral means spectrum for  $q + q' = 2p$ . In particular, the  $(p, 0)$  interior derivative moments studied in Ref. [9] correspond to the  $(p, 2p)$  mixed moments of the Beliaev–Smirnov exterior map.

Hence the general setting introduced in this work unifies the integral means spectrum studies of Refs. [3] and [9] in a broader framework, that also covers the  $p = q = q'$  logarithmic case, as well as the integral means of the map  $f$  (or  $\hat{f}$ ) itself, in the  $(0, q)$  (or  $(0, -q)$ ) case.

**6.2. Modified One-Point Function.** Let us now consider the *modified* SLE moduli one-point function,

$$(68) \quad F(z, \bar{z}) := \frac{1}{|z|^q} G(z, \bar{z}) = \mathbb{E} \left( \frac{|f'(z)|^p}{|f(z)|^q} \right).$$

Because of Eq. (57), it obeys the modified PDE,

$$(69) \quad \begin{aligned} \mathcal{P}(D)[F(z, \bar{z})] = & -\frac{\kappa}{2}(z\partial - \bar{z}\bar{\partial})^2 F - \frac{1+z}{1-z}z\partial F - \frac{1+\bar{z}}{1-\bar{z}}\bar{z}\bar{\partial}F \\ & + \left[ -\frac{p}{(1-z)^2} - \frac{p}{(1-\bar{z})^2} + 2p - q \right] F(z, \bar{z}) = 0, \end{aligned}$$

which, of course, differs from Eq. (57). We can rewrite it as

$$(70) \quad \begin{aligned} \mathcal{P}(D)[F(z, \bar{z})] = & -\frac{\kappa}{2}(z\partial - \bar{z}\bar{\partial})^2 F - \frac{1+z}{1-z}z\partial F - \frac{1+\bar{z}}{1-\bar{z}}\bar{z}\bar{\partial}F \\ & - p \left[ \frac{1}{(1-z)^2} + \frac{1}{(1-\bar{z})^2} + \sigma - 1 \right] F = 0, \end{aligned}$$

in term of the important new parameter,

$$(71) \quad \sigma := q/p - 1.$$

This PDE then exactly coincides with Eq. (106) in Ref. [9], where  $\sigma$  was meant to represent  $\pm 1$ , whereas here  $\sigma \in \mathbb{R}$ .

The value  $\sigma = +1$  corresponds to the original Beliaev–Smirnov case, where the integral means spectrum successively involves three functions [3]:

$$(72) \quad \beta_{\text{tip}}(p, \kappa) := -p - 1 + \frac{1}{4}(4 + \kappa - \sqrt{(4 + \kappa)^2 - 8\kappa p}),$$

$$(73) \quad \text{for } p \leq p'_0(\kappa) := -1 - \frac{3\kappa}{8};$$

$$(74) \quad \beta_0(p, \kappa) := -p + \frac{4 + \kappa}{4\kappa}(4 + \kappa - \sqrt{(4 + \kappa)^2 - 8\kappa p}),$$

for  $p'_0(\kappa) \leq p \leq p_0(\kappa)$ ;

$$(75) \quad \beta_{\text{lin}}(p, \kappa) := p - \frac{(4 + \kappa)^2}{16\kappa},$$

$$(76) \quad \text{for } p \geq p_0(\kappa) := \frac{3(4 + \kappa)^2}{32\kappa}.$$

As shown in Refs. [9, 18, 19, 20] in the  $\sigma = -1$  interior case, because of the unboundedness of the interior whole-plane SLE map, there exists a phase transition at  $p = p^*(\kappa)$ , with

$$(77) \quad \begin{aligned} p^*(\kappa) &:= \frac{1}{16\kappa} \left( (4 + \kappa)^2 - 4 - 2\sqrt{2(4 + \kappa)^2 + 4} \right) \\ &= \frac{1}{32\kappa} \left( \sqrt{2(4 + \kappa)^2 + 4} - 6 \right) \left( \sqrt{2(4 + \kappa)^2 + 4} + 2 \right). \end{aligned}$$

The integral means spectrum is afterwards given by

$$(78) \quad \beta(p, \kappa) := 3p - \frac{1}{2} - \frac{1}{2}\sqrt{1 + 2\kappa p}, \text{ for } p \geq p^*(\kappa).$$

Since  $p^*(\kappa) < p_0(\kappa)$  (76), this transition precedes and supersedes the transition from the bulk spectrum (74) towards the linear behavior (75).

The singularity analysis given in Ref. [9] led us to introduce the  $\sigma$ -dependent function

$$(79) \quad \beta_+^\sigma(p, \kappa) = (1 - 2\sigma)p - \frac{1}{2}(1 + \sqrt{1 - 2\sigma\kappa p}).$$

For  $\sigma = -1$ , it recovers the integral means spectrum (78) above for the interior whole-plane SLE, while for  $\sigma = +1$  it introduces a new spectrum,

$$(80) \quad \beta_+^{(+1)}(p, \kappa) = -p - \frac{1}{2}(1 + \sqrt{1 - 2\kappa p}),$$

the relevance of which for the exterior whole-plane SLE case is analyzed in a joint work of two of us with D. Beliaev [2].

For general real values of  $\sigma$  (71), we can rewrite (79) as a function of  $(p, q, \kappa)$ ,

$$(81) \quad \beta_+^\sigma(p, \kappa) = \beta_1(p, q; \kappa) := 3p - 2q - \frac{1}{2} - \frac{1}{2}\sqrt{1 + 2\kappa(p - q)}.$$

We claim that the spectrum generated by the integral means (64) in the general  $(p, q)$  case will involve the standard multifractal spectra (72), (74), (75), that are

independent of  $q$ , and also the new  $(p, q)$ -dependent multifractal spectrum (81). Phase transitions between these spectra will occur along lines drawn in the real  $(p, q)$  plane. The main reason for the occurrence of (81), to be presented in a future work, is that the analysis performed in Ref. [9], Section 4, for determining the integral means spectrum, in particular the range of validity of (79) and the corresponding proofs, can be adapted for general values of the  $\sigma$  parameter.

Here, we shall simply describe the corresponding partition of the  $(p, q)$  plane into the respective domains of validity of the four spectra above. We thus need to determine the boundary curves where pairs (possibly triplets) of these spectra coincide, which are signaling the onset of the respective transitions.

**6.3. Phase transition lines.** The best way is perhaps to recall the analytical derivation of the various multifractal spectra as done in Ref. [9], which was based on the use of functions  $A$  (38),  $B$  (39) and  $C$  (40). It will be convenient to use the notation [9],

$$(82) \quad A^\sigma(p, \gamma) := -\frac{\kappa}{2}\gamma^2 + \gamma - \sigma p,$$

such that for  $\sigma = q/p - 1$  (71),

$$(83) \quad A^\sigma(p, \gamma) = A(p, q; \gamma) = p - q + \gamma - \frac{\kappa}{2}\gamma^2,$$

as well as

$$(84) \quad B(q, \gamma) = q - \left(3 + \frac{\kappa}{2}\right)\gamma + \kappa\gamma^2,$$

$$(85) \quad C(p, \gamma) = -\frac{\kappa}{2}\gamma^2 + \left(2 + \frac{\kappa}{2}\right)\gamma - p,$$

$$(86) \quad \beta(p, \gamma) := \frac{\kappa}{2}\gamma^2 - C(p, \gamma) = \kappa\gamma^2 - \left(2 + \frac{\kappa}{2}\right)\gamma + p,$$

where the last function,  $\beta(p, \gamma)$ , is the so-called ‘‘spectrum function’’ [9]. Recall also that this function possesses an important duality property [9],

$$(87) \quad \beta(p, \gamma) = \beta(p, \gamma'), \quad \gamma + \gamma' := \frac{2}{\kappa} + \frac{1}{2}.$$

*Remark 6.2.* The B–S spectrum parameter  $\gamma_0$ , and bulk spectrum (74)  $\beta_0 := \beta(p, \gamma_0)$ , (corresponding to Eqs. (11) and (12) in Ref. [3]) are obtained from the equations (see Ref. [9]),

$$(88) \quad C(p, \gamma_0) = 0; \quad \beta_0 = \beta(p, \gamma_0) = \kappa\gamma_0^2/2.$$

The two solutions to (88) are  $\gamma_0^\pm(p)$  as in Eq. (26), where the lower branch  $\gamma_0 := \gamma_0^-$  is the one selected for the bulk spectrum,  $\beta_0(p) = \frac{1}{2}\kappa\gamma_0^-(p)^2$ .

This spectrum (74) is defined only to the *left* of a vertical line in the  $(p, q)$  plane, as given by (see Fig. 3)

$$(89) \quad \Delta_0 := \left\{ p = \frac{(4 + \kappa)^2}{8\kappa}, q \in \mathbb{R} \right\}.$$

*Remark 6.3.* The  $\sigma$ -dependent spectrum (79) is obtained from the equations

$$(90) \quad A^\sigma(p, \gamma) = 0; \quad \beta(p, \gamma) = \kappa\gamma^2/2 - C(p, \gamma).$$

The solutions to Eq. (90) are

$$(91) \quad \gamma_\pm^\sigma(p) = \frac{1}{\kappa}(1 \pm \sqrt{1 - 2\sigma\kappa p}),$$

$$(92) \quad \beta_\pm^\sigma(p) = (1 - 2\sigma)p - \frac{\kappa}{2}\gamma_\pm^\sigma(p) = (1 - 2\sigma)p - \frac{1}{2}(1 \pm \sqrt{1 - 2\sigma\kappa p}).$$

The multifractal spectrum (79) is then given by the upper branch  $\beta_+^\sigma(p)$  [9]. Note also that this spectrum is defined only for  $2\sigma\kappa p \leq 1$ , hence for points in the  $(p, q)$  plane *below* the oblique line (Fig. 3):

$$(93) \quad \Delta_1 := \{(p, q) \in \mathbb{R}^2, q = p + 1/2\kappa\}.$$

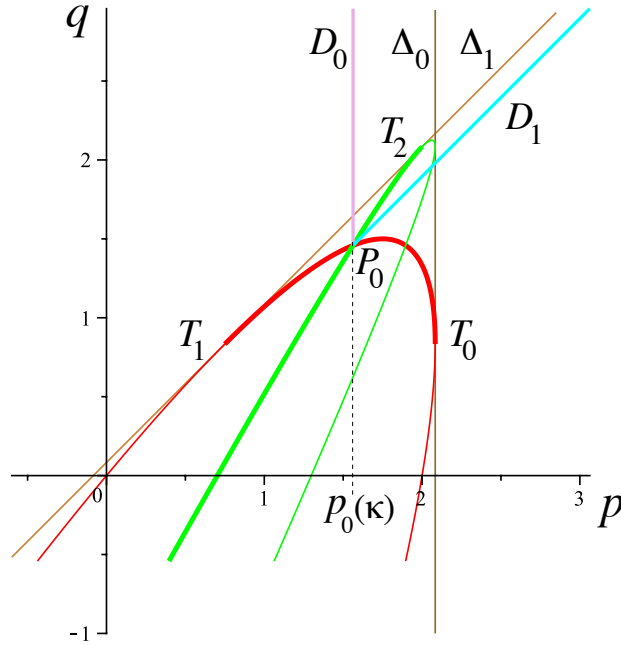


FIGURE 3. Red parabola  $\mathcal{R}$  (95) and green parabola  $\mathcal{G}$  (98) (for  $\kappa = 6$ ). From the intersection point  $P_0$  (100) originate the two (half)-lines  $D_0$  (102) and  $D_1$  (103). The bulk spectrum  $\beta_0(p)$  and the generalized spectrum  $\beta_1(p, q)$  coincide along the arc (96) of red parabola between its tangency points  $T_0$  and  $T_1$  with  $\Delta_0$  and  $\Delta_1$  (thick red line). They also coincide along the infinite left branch (99) of the green parabola, up to its tangency point  $T_2$  to  $\Delta_1$  (thick green line). The  $\beta_0(p)$  spectrum and the linear one  $\beta_{\text{lin}}(p)$  coincide along  $D_0$ , whereas  $\beta_1(p, q)$  and  $\beta_{\text{lin}}(p)$  coincide along  $D_1$ .



6.3.1. *The Red Parabola.* The parabola  $\mathcal{R}$  of Theorems 3.1 and 4.2, which we shall hereafter call (and draw in) **red** (see Fig. 3), is given by the simultaneous conditions,

$$(94) \quad A^\sigma(p, \gamma) = A(p, q, \gamma) = 0, \quad C(p, \gamma) = 0,$$

hence also  $B(q, \gamma) = 0$ , which recovers the parametric form (24)

$$(95) \quad \begin{aligned} p &= p_{\mathcal{R}}(\gamma) := \left(2 + \frac{\kappa}{2}\right) \gamma - \frac{\kappa}{2} \gamma^2, \\ q &= q_{\mathcal{R}}(\gamma) := \left(3 + \frac{\kappa}{2}\right) \gamma - \kappa \gamma^2, \quad \gamma \in \mathbb{R}. \end{aligned}$$

By construction, the associated spectrum  $\beta(p, \gamma)$  is therefore both of the B–S type,  $\beta_0^\pm(p)$ , and of the novel type,  $\beta_\pm^\sigma(p)$ . We successively have:

$$(96) \quad \begin{aligned} \gamma &= \gamma_-^\sigma(p) = \gamma_0^-(p); \quad \beta_-^\sigma(p) = \beta_0^-(p), \quad \gamma \in (-\infty, 1/\kappa], \\ \gamma &= \gamma_+^\sigma(p) = \gamma_0^-(p); \quad \beta_+^\sigma(p) = \beta_0^-(p), \quad \gamma \in [1/\kappa, 2/\kappa + 1/2], \\ \gamma &= \gamma_+^\sigma(p) = \gamma_0^+(p); \quad \beta_+^\sigma(p) = \beta_0^+(p), \quad \gamma \in [2/\kappa + 1/2, +\infty), \end{aligned}$$

where the change of analytic branch from the first to the second line corresponds to a tangency at  $T_1$  of the red parabola to the boundary line  $\Delta_1$ , whereas the change from second to third corresponds to a tangency at  $T_0$  to the vertical boundary line  $\Delta_0$ . The interval where the multifractal spectra coincide, i.e., when  $\beta_+^\sigma(p) = \beta_0^-(p)$ , is thus given by line (96) in the equations above.

In Cartesian coordinates, the red parabola  $\mathcal{R}$  (95) has for equation (25).

6.3.2. *The Green Parabola.* A second parabola in the  $(p, q)$  plane, hereafter called **green** (see Fig. 3) and denoted by  $\mathcal{G}$ , is such that the multifractal spectra  $\beta_0^-(p)$  and  $\beta_+^\sigma(p) = \beta(p, q; \kappa)$  coincide on part of it. We use the *duality* property (87) of the spectrum function [9], and set the simultaneous seed conditions,

$$(97) \quad \begin{aligned} A^\sigma(p, \gamma') &= A(p, q, \gamma') = 0, \quad C(p, \gamma'') = 0, \\ \gamma' + \gamma'' &= 2/\kappa + 1/2, \end{aligned}$$

where  $\gamma'$  and  $\gamma''$  are *dual* of each other and such that  $\beta(p, \gamma') = \beta(p, \gamma'')$ .

Eqs. (38) and (40) immediately give the parametric form for the green parabola,

$$(98) \quad \begin{aligned} p &= p_{\mathcal{G}}(\gamma') := \frac{(4 + \kappa)^2}{8\kappa} - \frac{\kappa}{2} \gamma'^2, \\ q &= q_{\mathcal{G}}(\gamma') := \frac{(4 + \kappa)^2}{8\kappa} + \gamma' - \kappa \gamma'^2, \quad \gamma' \in \mathbb{R}. \end{aligned}$$

Along this locus, we successively have:

$$(99) \quad \begin{aligned} \gamma' &= \gamma_-^\sigma(p), \gamma'' = \gamma_0^+(p); \quad \beta_-^\sigma(p) = \beta_0^+(p), \quad \gamma' \in (-\infty, 0], \\ \gamma' &= \gamma_-^\sigma(p), \gamma'' = \gamma_0^-(p); \quad \beta_-^\sigma(p) = \beta_0^-(p), \quad \gamma' \in [0, \kappa^{-1}], \\ \gamma' &= \gamma_+^\sigma(p), \gamma'' = \gamma_0^-(p); \quad \beta_+^\sigma(p) = \beta_0^-(p), \quad \gamma' \in [\kappa^{-1}, +\infty), \end{aligned}$$

where the changes of branches correspond to a tangency of the green parabola to  $\Delta_0$  followed by a tangency to  $\Delta_1$ . The multifractal spectra coincide when  $\beta_+^\sigma(p) = \beta_0^-(p)$ , which corresponds to the third line (99) in the equations above, i.e., to the domain where  $\gamma' \geq 1/\kappa$ .

6.3.3. *Quadruple point.* The intersection of the red and green parabolae (95) and (98) can be found by combining the seed equations (94) and (97). We find either  $\gamma = \gamma' = 1/\kappa + 1/4$ , or  $\gamma = 2/\kappa + 1/4, \gamma' = -1/4$ , which lead to the two intersection points,

$$(100) \quad P_0 : p_0 = p_0(\kappa) = \frac{3(4 + \kappa)^2}{32\kappa}, \quad q_0 = \frac{(4 + \kappa)(8 + \kappa)}{16\kappa},$$

$$(101) \quad P_1 : p_1 = \frac{(8 + \kappa)(8 + 3\kappa)}{32\kappa}, \quad q_0 = \frac{(4 + \kappa)(8 + \kappa)}{16\kappa}.$$

Note that these points have same ordinate, while the abscissa of the left-most one,  $P_0$ , is  $p_0(\kappa)$  (76), where the integral means spectrum transits from the B–S bulk form (74) to its linear form (75).

Through this intersection point  $P_0$  further pass two important straight lines in the  $(p, q)$  plane.

**Definition 6.4.**  $D_0$  and  $D_1$  are, respectively, the vertical line and the slope one line passing through point  $P_0$ , of equations

$$(102) \quad D_0 := \{(p, q) : p = p_0\},$$

$$(103) \quad D_1 := \left\{ (p, q) : q - p = q_0 - p_0 = \frac{16 - \kappa^2}{32\kappa} \right\}.$$

A key property of  $D_1$  is the following. The difference,

$$(104) \quad \beta_1(p, q; \kappa) - \beta_{\text{lin}}(p, \kappa) = \frac{1}{\kappa} \left( \frac{\kappa}{4} - \sqrt{1 + 2\kappa(p - q)} \right)^2,$$

is always positive, and vanishes only on line  $D_1$ , where

$$(105) \quad \forall (p, q) \in D_1, \quad \beta_1(p, q; \kappa) = \beta_{\text{lin}}(p, \kappa) = p - \frac{(4 + \kappa)^2}{16\kappa}.$$

6.3.4. *The Blue Quartic.* A third locus, the **blue** quartic  $\mathcal{Q}$ , will also play an important role, that is where the B–S tip-spectrum,  $\beta_{\text{tip}}(p; \kappa)$  (72), coincides with the novel spectrum,  $\beta_+^\sigma(p) = \beta_1(p, q; \kappa)$ . The tip spectrum is given by  $\beta_{\text{tip}}(p; \kappa) = \beta(p, \gamma_0) - 2\gamma_0 - 1$ , where  $\gamma_0$  is solution to  $C(p, \gamma_0) = 0$  and such that the tip contribution is positive,  $2\gamma_0 + 1 \leq 0$  [3, 9]; this corresponds to the tip condition (73) [3]. In the  $(p, q)$  plane, this describes the domain to the left of the straight line  $D'_0$  (Fig. 4), defined by

$$(106) \quad D'_0 := \{(p, q) : p = p'_0(\kappa) = -1 - 3\kappa/8\}.$$

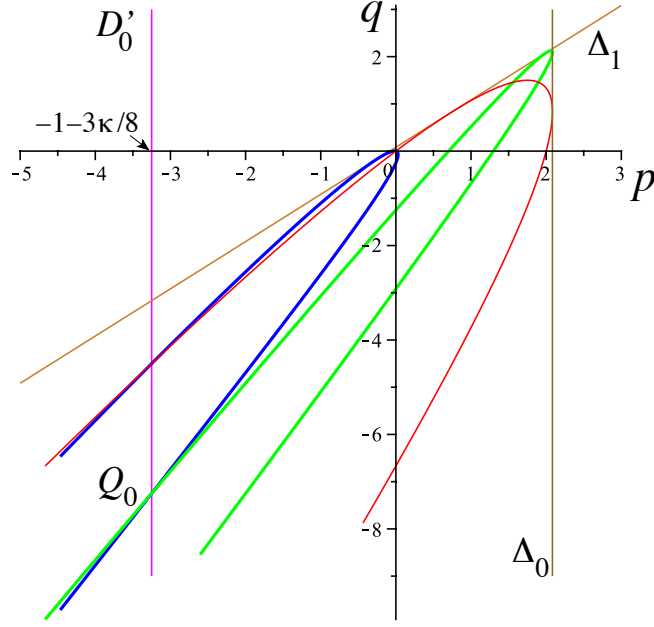


FIGURE 4. The blue quartic 113 for  $\kappa = 6$ . It intersects the green parabola at point  $Q_0$  (117) and the red parabola at point  $Q_1$  (116) (not marked), both of abscissa  $p'_0(\kappa) = -1 - 3\kappa/8$ .

The generalized spectrum is given by  $\beta_{\pm}^{\sigma}(p) = \beta(p, \gamma)$  where  $\gamma$  is solution to  $A^{\sigma}(p, \gamma) = 0$ . We therefore look for simultaneous solutions to the seed equations,

$$(107) \quad \begin{aligned} \beta(p, \gamma) &= \beta(p, \gamma_0) - 2\gamma_0 - 1, \quad 2\gamma_0 + 1 \leq 0, \\ A^{\sigma}(p, \gamma) &= 0, \quad C(p, \gamma_0) = 0. \end{aligned}$$

Using Eq. (83), we first find, as for the red and green parabolae,

$$(108) \quad q - p = \gamma - \frac{\kappa}{2}\gamma^2,$$

and from (86) and (85), by substitution in the above,

$$(109) \quad 2p - q + \frac{1}{2} = \frac{\kappa}{4}(\gamma + \gamma_0),$$

$$(110) \quad \frac{4 + \kappa}{2}\gamma - \kappa\gamma^2 - 1 = \frac{8 + \kappa}{2}\gamma_0 - \kappa\gamma_0^2.$$

Solving for  $\gamma_0$  in terms of  $\gamma$  gives

$$(111) \quad \gamma_0 = \gamma_0^{\pm} := \frac{8 + \kappa}{4\kappa} \pm \frac{1}{2\kappa}\Delta^{\frac{1}{2}}(\gamma),$$

$$(112) \quad \Delta(\gamma) := 4\kappa^2\gamma^2 - 2\kappa(4 + \kappa)\gamma + \frac{1}{4}(8 + \kappa)^2 + 4\kappa,$$

with  $\Delta(\gamma) > 0, \forall \gamma \in \mathbb{R}$ . The tip relevance inequality in (107),  $2\gamma_0 + 1 \leq 0$ , implies the choice of the negative branch in (111):  $\gamma_0 = \gamma_0^-$ . We thus get the desired explicit parameterization of that branch of the quartic,

$$(113) \quad \begin{aligned} p &= p_{\mathcal{Q}}(\gamma) := \frac{\kappa}{16} + \left(1 + \frac{\kappa}{4}\right) \gamma - \frac{\kappa}{2} \gamma^2 - \frac{1}{8} \Delta^{\frac{1}{2}}(\gamma), \\ q &= q_{\mathcal{Q}}(\gamma) := p_{\mathcal{Q}}(\gamma) + \gamma - \frac{\kappa}{2} \gamma^2, \quad \gamma \in \mathbb{R}. \end{aligned}$$

*Remark 6.5.* Note that because of the very choice to parameterize the parabolae and the quartic by  $\gamma$ , such that  $A$  (83) vanishes, Eq. (108) holds for each of the pairs of parametric equations.

We successively have along the branch (113) of the blue quartic:

$$(114) \quad \begin{aligned} \gamma &= \gamma_-^\sigma(p); \quad \beta_-^\sigma(p) = \beta_{\text{tip}}(p), \gamma \in (-\infty, 1/\kappa], \\ \gamma &= \gamma_+^\sigma(p); \quad \beta_+^\sigma(p) = \beta_{\text{tip}}(p) < \beta_0^-(p), \gamma \in [1/\kappa, 1 + 2/\kappa], \end{aligned}$$

$$(115) \quad \gamma = \gamma_+^\sigma(p); \quad \beta_+^\sigma(p) = \beta_{\text{tip}}(p) \geq \beta_0^-(p), \gamma \in [1 + 2/\kappa, +\infty),$$

The intersection of the **blue** quartic (113) with the **red** parabola  $\mathcal{R}$  (95) is located at

$$(116) \quad Q_1 : p'_0 = -1 - \frac{3\kappa}{8}, q = -\frac{1}{2}(3 + \kappa); \quad \gamma = \gamma_0 = -\frac{1}{2},$$

followed by a second intersection at the origin,  $p = q = 0$ , for  $\gamma = \frac{2}{\kappa}$  and  $\gamma_0 = 0$ .

The intersection of the **blue** quartic (113) with the **green** parabola  $\mathcal{G}$  (98) is located at

$$(117) \quad Q_0 : p'_0 = -1 - \frac{3\kappa}{8}, q'_0 := -2 - \frac{7\kappa}{8}; \quad \gamma = \gamma' = 1 + \frac{2}{\kappa}, \gamma_0 = -\frac{1}{2}.$$

Notice that these two intersection points have same abscissae,  $p'_0(\kappa)$  (73), where the transition for  $\gamma_0 = -\frac{1}{2}$  from the B–S bulk spectrum to the tip spectrum takes place. They are found by combining Eqs. (94) or Eqs. (97) with (107).

The tip spectrum and the generalized one coincide in both  $\gamma$ -intervals (114) and (115), which together parameterize the branch of the quartic located below its contact with  $\Delta_1$  (see Fig. 4). Because of the tip relevance condition (73), only the interval (115) describing the lower infinite branch of the quartic located to the *left* of  $Q_0$  will matter for the integral means spectrum.

#### 6.4. Whole-plane $\text{SLE}_\kappa$ generalized spectrum.

6.4.1. *Summary.* Let us briefly summarize the results of Section 6.3. We know from Eq. (96) that the B–S bulk spectrum  $\beta_0(p)$  and the mixed spectrum  $\beta_1(p, q)$  coincide along the finite sector of parabola  $\mathcal{R}$  located between tangency points  $T_0$  and  $T_1$  (Fig. 3). From Eq. (99), we also know that they coincide along the infinite left branch of parabola  $\mathcal{G}$  below the tangency point  $T_2$  (Fig. 3).

The linear bulk spectrum  $\beta_{\text{lin}}(p)$  coincides with  $\beta_0(p)$  along line  $D_0$  and supersedes the latter to the right of  $D_0$  (Fig. 3). We know from (105) that  $\beta_{\text{lin}}(p)$  and  $\beta_1(p, q)$  coincide along the line  $D_1$  (Fig. 3).

The tip spectrum  $\beta_{\text{tip}}(p)$  coincides with  $\beta_0(p)$  along line  $D'_0$ , and supersedes it to the left of  $D'_0$ . We finally know from Eq. (115) that this tip spectrum  $\beta_{\text{tip}}(p)$  coincides with  $\beta_1(p, q)$  along the lower branch of the blue quartic located below point  $Q_0$  (117) (Fig. 4).

The only possible scenario which thus emerges to construct the average generalized integral means spectrum by a continuous matching of the 4 different spectra along the phase transition lines described above, is the partition of the  $(p, q)$  plane in 4 different regions as indicated in Fig. 5:

- a part (I) to the left of  $D'_0$  and located above the blue quartic up to point  $Q_0$ , where the average integral means spectrum is  $\beta_{\text{tip}}(p)$ ;
- an upper part (II) bounded by lines  $D'_0$ ,  $D_0$ , and located above the section of the green parabola between points  $Q_0$  and  $P_0$ , where the spectrum is given by  $\beta_0(p)$ ;
- an infinite wedge (III) of apex  $P_0$  located between the upper half-lines  $D_0$  and  $D_1$ , where the spectrum is given by  $\beta_{\text{lin}}(p)$ ;
- a lower part (IV) whose boundary is the blue quartic up to point  $Q_0$ , followed by the arc of green parabola between points  $Q_0$  and  $P_0$ , followed by the half-line  $D_1$  above  $P_0$  where the spectrum is  $\beta_1(p, q)$ .

The two wings  $T_1P_0$  and  $P_0T_0$  of the red parabola (Fig. 3), where we know from Theorem 4.2 that the average spectrum is given by  $\beta_0(p) = \beta_1(p, q)$ , can thus be seen as the respective extensions of region IV into II and of region II into IV.

This is summarized by the following proposition.

**Proposition 6.1.** *The separatrix curves for the generalized integral means spectrum of whole-plane SLE $_{\kappa}$  are in the  $(p, q)$  plane (Fig. 5):*

- (i) the vertical half-line  $D_0$  above  $P_0 = (p_0, q_0)$  (100), where  $p_0 = 3(4 + \kappa)^2/32\kappa$ ,  $q_0 = (4 + \kappa)(8 + \kappa)/16\kappa$ ;
- (ii) the unit slope half-line  $D_1$  originating at  $P_0$ , whose equation is  $q - p = (16 - \kappa^2)/32\kappa$  with  $p \geq p_0$ ;
- (iii) the section of green parabola, with parametric coordinates  $(p_{\mathcal{G}}(\gamma), q_{\mathcal{G}}(\gamma))$  (98) for  $\gamma \in [1/4 + 1/\kappa, 1 + 2/\kappa]$ , between  $P_0$  and  $Q_0 = (p'_0, q'_0)$  (117), where  $p'_0 = -1 - 3\kappa/8$ ,  $q'_0 = -2 - 7\kappa/8$ ;
- (iv) the vertical half-line  $D'_0$  above point  $Q_0$ ;
- (v) the branch of the blue quartic from  $Q_0$  to  $\infty$ , with parametric coordinates  $(p_{\mathcal{Q}}(\gamma), q_{\mathcal{Q}}(\gamma))$  (113) for  $\gamma \in [1 + 2/\kappa, +\infty)$ .

6.4.2. *The B-S line.* As mentioned above, the whole-plane SLE case studied by Beliaev and Smirnov corresponds to the  $q = 2p$  line. Because of Eq. (25), it intersects the red parabola  $\mathcal{R}$  only at  $p = 0$ . The green parabola  $\mathcal{G}$  (98) has for

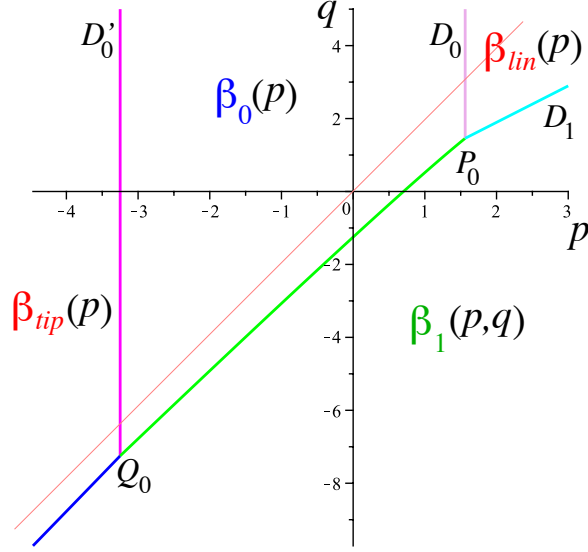


FIGURE 5. Respective domains of validity of integral means spectra  $\beta_{\text{tip}}(p)$ ,  $\beta_0(p)$ ,  $\beta_{\text{lin}}(p)$ , and  $\beta_1(p, q)$ . The thin straight line (coral)  $q = 2p$  corresponds to the version of whole-plane SLE studied in Ref. [3]. It does not intersect the lower domain where  $\beta_1$  holds.

Cartesian equation (see also Section 7),

$$(118) \quad \frac{\kappa}{2}(2p - q)^2 - \frac{1}{8}(4 + \kappa)^2(2p - q) + p + \frac{1}{128}(4 + \kappa)^2(8 + \kappa) = 0,$$

which shows that it intersects the the B–S line at [2]

$$(119) \quad p = p_0''(\kappa) := -\frac{1}{128}(4 + \kappa)^2(8 + \kappa),$$

which is to the *left* of the tip transition line at  $p_0'(\kappa) = -1 - \frac{3}{8}\kappa$  (73). The quartic  $\mathcal{Q}$  (113) obeys (see also Section 7)

$$(120) \quad \left[ \left( 2p - q - \frac{\kappa}{16} \right)^2 - \frac{c}{4} \right] \left( 2p - q - 1 - \frac{\kappa}{8} \right) (2p - q) = \frac{\kappa}{2}(p - q) \left( 2p - q - \frac{1}{4} - \frac{\kappa}{8} \right)^2$$

$$c = c(\kappa) := \frac{1}{64}(8 + \kappa)^2 + \frac{\kappa}{4},$$

which immediately shows that the B–S line  $q = 2p$  intersects  $\mathcal{Q}$  only at the origin and stays above its lower branch.

The B–S line therefore does not intersect the segment of green parabola  $\mathcal{G}$  between  $P_0$  and  $Q_0$ , nor the quartic  $\mathcal{Q}$  below  $Q_0$  (Fig. 5). Thus the novel spectrum  $\beta_1$  *does not* a priori appear in the version of whole-plane SLE considered in Ref. [3]. The B–S line nevertheless intersects  $\mathcal{G}$  at  $p_0''$  (119) to the left of  $Q_0$ ,

in a domain lying above the quartic and where the integral mean receives a non-vanishing contribution from the SLE tip. But if that integral mean is restricted to avoid a neighborhood of  $z = 1$ , whose image is the tip, only the bulk spectrum remains, and a phase transition will take place from  $\beta_0$  to  $\beta_1$  when the line  $q = 2p$  crosses  $\mathcal{G}$ . As we shall see in Section 6.5, the  $\beta_1$  spectrum can also directly appear in the averaged integral means spectra of higher  $m$ -fold transforms of the B–S version of whole-plane SLE.

6.4.3. *The Koebe  $\kappa \rightarrow 0$  limit.* In this limit, Eq. (25) of the red parabola  $\mathcal{R}$  becomes  $3p - 2q = 0$ , Eq. (118) of the green one  $\mathcal{G}$  becomes  $3p - 2q - 1 = 0$ , and Eq. (120) of the quartic factorizes into that of four parallel lines, among which  $q = 2p$  gives the relevant lower branch. Point  $P_0$  moves up to infinity, whereas  $Q_0 \rightarrow (-1, -2)$ . The phase diagram is thus made of only three different regions, I, where  $\beta_{\text{tip}}(p) = -p - 1$ , II, where  $\beta_0 = 0$ , and IV, where  $\beta_1(p, q) = 3p - 2q - 1$ .

6.4.4. *Checks.* The proposed partition of the  $(p, q)$  plane can be checked against several rigorous results [9]. The red parabola  $\mathcal{R}$  (95) is parameterized by  $\gamma$  (96) such that  $C(\gamma) = 0$ , where  $\gamma = \gamma_-^\sigma(p)$  before the tangency point  $T_1$ , and  $\gamma = \gamma_+^\sigma(p)$  after it (Fig. 3). It partitions the half-plane below  $\Delta_1$  into an open interior  $\mathcal{I}$  of  $\mathcal{R}$ , where  $C(\gamma_+^\sigma) > 0$  and  $C(\gamma_-^\sigma) < 0$ ; an open exterior  $\mathcal{E}_-$  located to the left of tangency point  $T_1$ , where  $C(\gamma_\pm^\sigma) > 0$ ; an open exterior  $\mathcal{E}_+$  to the right of  $T_1$ , where  $C(\gamma_\pm^\sigma) < 0$ .

According to Ref. [9], Section 4.2.5, and the generalization thereof to PDE (70), there exists then in  $\mathcal{I} \cup \mathcal{E}_-$  a supersolution to Eq. (70) of critical exponent  $\beta(\gamma_+^\sigma) = \beta_+^\sigma(p) = \beta_1(p, q)$ , such that the *true* average integral means spectrum, say  $\beta(p, q)$ , is bounded below as  $\beta(p, q) \geq \beta_1(p, q)$ , whereas there exists in  $\mathcal{E}_+$  a subsolution to (70) with the same critical exponent  $\beta(\gamma_+^\sigma) = \beta_1(p, q)$ , such that now  $\beta(p, q) \leq \beta_1(p, q)$ .

In region  $\mathcal{I}$ , and to the left of the thick branch of the green parabola below  $P_0$  (Fig. 3), we thus have  $\beta_1(p, q) < \beta_0(p)$  and  $\beta_1(p, q) \leq \beta(p, q)$ , which is consistent with  $\beta(p, q) = \beta_0(p)$  (Fig. 5). In region  $\mathcal{I}$ , and to the right of the thick branch of the green parabola below  $P_0$ , we by contrast have  $\beta_1(p, q) > \beta_0(p)$  still with  $\beta(p, q) \geq \beta_1(p, q)$ , in agreement with  $\beta(p, q) = \beta_1(p, q)$  there (Fig. 5).

In region  $\mathcal{E}_+$ , consider now the inside of the curved triangle  $T_1 P_0 T_2$  (Fig. 3), where  $\beta_1(p, q) > \beta_0(p) \geq \beta_{\text{lin}}(p)$ , and  $\beta_1(p, q) \geq \beta(p, q)$ ; this is consistent with  $\beta(p, q) = \beta_0(p)$  to the left of  $D_0$  and  $\beta(p, q) = \beta_{\text{lin}}(p)$  to the right of  $D_0$  (Fig. 5).

Consider the region in  $\mathcal{E}_+$  delimited by the arc  $P_0 T_0$  of the red parabola, the arc  $P_0 T_2$  of the green parabola, the half-line  $\Delta_1$  above  $T_2$  and the vertical line  $\Delta_0$  (Fig. 3); in this region one has  $\beta_{\text{lin}}(p) \leq \beta_1(p, q) \leq \beta_0(p)$ , together with the true spectrum  $\beta(p, q) \leq \beta_1(p, q)$ , and this is both consistent with the claims  $\beta(p, q) = \beta_1(p, q)$  below  $D_1$  and  $\beta(p, q) = \beta_{\text{lin}}(p)$  above  $D_1$  (Fig. 5).

In the band in  $\mathcal{E}_+$  between  $D_1$  and  $\Delta_1$  and to the left of  $\Delta_0$  (Fig. 3), we have both  $\beta_{\text{lin}}(p) \leq \beta_1(p, q)$  and  $\beta(p, q) \leq \beta_1(p, q)$ , which is consistent with  $\beta(p, q) = \beta_{\text{lin}}(p)$  there (Fig. 5). In the remainder of the angular sector above  $\Delta_1$

and to the right of  $D_0$ , the function  $\beta_1$  is no longer defined, and we are left with the usual linear spectrum  $\beta_{\text{lin}}(p) = \beta(p, q)$  as the only possibility (Fig. 5).

In the part of region  $\mathcal{E}_+$ , with the shape of a curved wedge located in between the branch of red parabola below  $T_0$  and the half-line  $\Delta_0$  below  $T_0$  (Fig. 3), we have  $\beta_0(p) \leq \beta_1(p, q)$  and  $\beta(p, q) \leq \beta_1(p, q)$  which is consistent with the claim  $\beta(p, q) = \beta_1(p, q)$  in this region (Fig. 5). To the right of  $\Delta_0$  and below  $D_1$ , the function  $\beta_0$  is no longer defined, and we are left with  $\beta(p, q) = \beta_1(p, q)$  as the only possibility (Fig. 5).

Consider now, in the region to the right of the vertical line  $D'_0$  (Fig. 4), the union of the exterior sector  $\mathcal{E}_-$  and of the open part of  $\mathcal{I}$  located to the left of the green parabola: there  $\beta_1(p, q) < \beta_0(p)$ , while we know that  $\beta_1(p, q) \leq \beta(p, q)$ , which is consistent with the prediction that the true spectrum there is  $\beta_0(p)$  (Fig. 5).

Finally, consider the tip region to the left of the vertical line  $D'_0$  (Fig. 4); the lowest part of this region lies in the exterior part  $\mathcal{E}_+$  where  $\beta(p, q) \leq \beta_1(p, q)$ , followed by a part intersecting  $\mathcal{I} \cup \mathcal{E}_-$  where  $\beta(p, q) \geq \beta_1(p, q)$ , and ending with a domain above  $\Delta_1$ . We have along the branch  $\mathcal{Q}$  of the blue quartic drawn below its intersection point  $Q_0$  with the green parabola,  $\beta_{\text{tip}}(p) = \beta_1(p, q)$ ; below it,  $\beta_0(p) < \beta_{\text{tip}}(p) < \beta_1(p, q)$ ; above it,  $\beta_1(p, q) < \beta_{\text{tip}}(p)$ . All this is consistent with the claim  $\beta(p, q) = \beta_1(p, q)$  below  $\mathcal{Q}$  and  $\beta(p, q) = \beta_{\text{tip}}(p)$  in  $\mathcal{I} \cup \mathcal{E}_-$  above  $\mathcal{Q}$  (Fig. 5). Finally, in the domain above  $\Delta_1$ , the function  $\beta_1$  no longer exists and we are left with  $\beta(p, q) = \beta_{\text{tip}}(p) > \beta_0(p)$  as the only possibility for the average integral means spectrum (Fig. 5).

**6.5.  $m$ -fold spectrum.** The generalized integral means spectrum  $\beta^{[m]}(p, q; \kappa)$ , associated with the  $m$ -fold transform  $f^{[m]}$  of the SLE whole-plane map, can be directly derived from the analysis given in Section 5. Identities (58) and (59) immediately imply that

$$(121) \quad \begin{aligned} \beta^{[m]}(p, q; \kappa) &= \beta^{[1]}(p, q_m; \kappa), \\ q_m = q_m(p, q) &= (1 - 1/m)p + q/m, \end{aligned}$$

where  $\beta^{[1]}(p, q; \kappa) = \beta(p, q; \kappa)$  is the  $m = 1$  averaged integral means spectrum of whole-plane  $\text{SLE}_\kappa$  studied above.

Let  $T_m = \begin{pmatrix} 1 & 0 \\ 1-1/m & 1/m \end{pmatrix}$  be the endomorphism of  $\mathbb{R}^2$  given by  $T_m(p, q) = (p, q_m)$ , with inverse  $T_m^{-1} = \begin{pmatrix} 1 & 0 \\ 1-m & m \end{pmatrix}$ . Then the separatrix lines for the  $m$ -fold case are the images by  $T_m^{-1}$  of those for  $m = 1$ . Proposition 6.1 then yields:

**Proposition 6.2.** *(Figure 6) The separatrix curves for the generalized integral means spectrum of the  $m$ -fold whole-plane  $\text{SLE}_\kappa$  are given, for  $m \geq 1$ , by the same as in Proposition 6.1 for  $m = 1$ , provided that one replaces there,*

- $D_0$  by  $D_0^{[m]}$ ,  $P_0$  by  $P_0^{[m]}$ ,  $q_0$  by  $q_0^{[m]} := p_0 + m(16 - \kappa^2)/32\kappa$ ;
- $D_1$  by  $D_1^{[m]}$ , with  $q - p = m(16 - \kappa^2)/32\kappa$ ;
- $q_G(\gamma)$  by  $p_G(\gamma) + m(\gamma - \kappa\gamma^2/2)$ ,  $Q_0$  by  $Q_0^{[m]}$ ,  $q'_0$  by  $q_0'^{[m]} := p'_0 - m(1 + \kappa/2)$ ;



- $D'_0$  by  $D_0^{[m]}$ ;
- $q_{\mathcal{Q}}(\gamma)$  by  $p_{\mathcal{Q}}(\gamma) + m(\gamma - \kappa\gamma^2/2)$ .

For  $m \leq -1$ , the same conclusions hold, except that, because  $\det T_m^{-1} = m < 0$ , the vertical positions of the respective domains of validity of the spectra are all *reversed*, the vertical separatrix lines  $D_0^{[m]}$  and  $D_0'^{[m]}$  being now half-lines going from *below*  $P_0^{[m]}$  and  $Q_0^{[m]}$  to  $-\infty$ , and the domain IV lying *above* the half-line  $D_1^{[m]}$ , the transformed green parabola and the transformed quartic. The concavity of the separatrix curves is correspondingly inverted (Fig. 6, right).

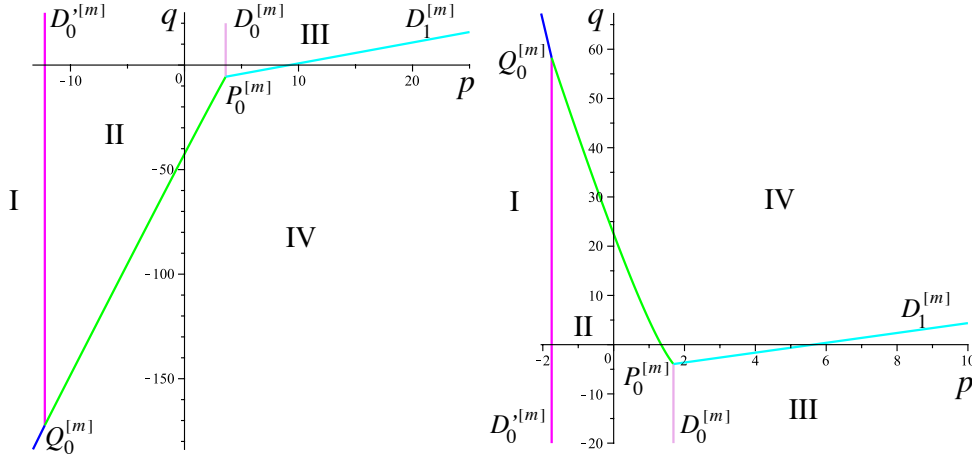


FIGURE 6. Phase diagram for the  $m$ -fold whole-plane  $\text{SLE}_\kappa$  and domains of validity of spectra  $\beta_{\text{tip}}$  (I),  $\beta_0$  (II),  $\beta_{\text{lin}}$  (III), and  $\beta_m$  (IV). Left: For  $m = +10$  and  $\kappa = 30$ , the  $q = 0$  line crosses successively domains I, II, III and IV. Right: For  $m = -30$  and  $\kappa = 2$ , this line crosses successively domains I, II, IV and III.

The allure of the  $m$ -separatrices are easily deduced from Proposition 6.2; in particular, the transformed quartic is asymptotic for  $p \rightarrow -\infty$  to a straightline,

$$q = (m + 1)p - m(2 + \kappa)/8,$$

whose direction is also that of the axis of the transform of the green parabola  $\mathcal{G}$ . Note the slope inversion when going from  $m \geq 1$  to  $m \leq -1$ . The  $m = -1$  case, i.e., the B–S version of whole-plane SLE, is thus peculiar: the parabola’s axis and the quartic’s linear asymptote are both horizontal, and  $\mathcal{G}$  intersects the  $p$ -axis at  $p_0''(\kappa) \leq p_0'(\kappa)$ , in agreement with Section 6.4.2. (See Fig. 7.)

In region IV, the  $m$ -fold integral means spectrum is thus given by

$$(122) \quad \begin{aligned} \beta^{[m]}(p, q; \kappa) &= \beta_m(p, q; \kappa) := \beta_1(p, q_m; \kappa) \\ &= \left(1 + \frac{2}{m}\right)p - \frac{2}{m}q - \frac{1}{2} - \frac{1}{2}\sqrt{1 + \frac{2\kappa}{m}(p - q)}. \end{aligned}$$

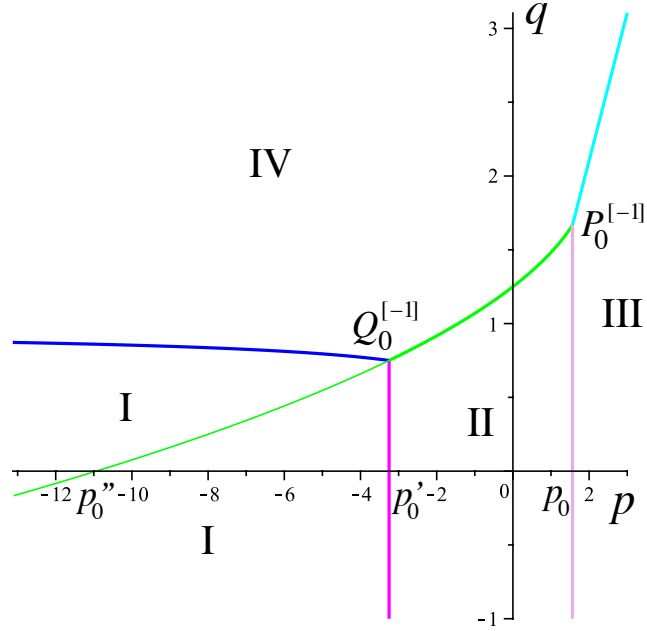


FIGURE 7. Phase diagram for the  $m = -1$  case. (Here  $\kappa = 6$ .)

Let us focus hereafter on the standard  $q = 0$  case for the  $m$ -fold spectrum. It yields

$$(123) \quad \begin{aligned} \beta_m(p, q = 0; \kappa) &= \beta_1(p, (1 - 1/m)p; \kappa) \\ &= \left(1 + \frac{2}{m}\right)p - \frac{1}{2} - \frac{1}{2}\sqrt{1 + \frac{2\kappa p}{m}}, \end{aligned}$$

in agreement with the result obtained in [Ref. [9], Eq. (22)].

In Proposition 6.2, observe now that the coordinate  $q_0^{[m]}$  of point  $P_0^{[m]}$  can become *negative*. In that case, the  $q = 0$  axis intersects the four different regions for the  $m$ -fold spectrum (Fig. 6). This happens for

$$(124) \quad m \frac{1}{3} \frac{\kappa - 4}{\kappa + 4} \geq 1,$$

which in turn splits into two possibilities, either  $\kappa > 4, m > 0$ , or  $\kappa < 4, m < 0$ .

In the first case, when  $p$  describes the entire real line, we get the sequence of spectra,  $\beta_{\text{tip}}, \beta_0, \beta_{\text{lin}}$ , and finally  $\beta_m$ , in agreement with [Ref. [9], Eqs. (26)-(29)]. In the second one, we get the sequence of spectra,  $\beta_{\text{tip}}, \beta_0, \beta_m$ , and finally  $\beta_{\text{lin}}$  (Fig. 6).

The same conclusions can be obtained by working with the r.h.s. of (123), i.e., by following the line

$$(125) \quad q = q_m(p, 0) = (1 - 1/m)p,$$

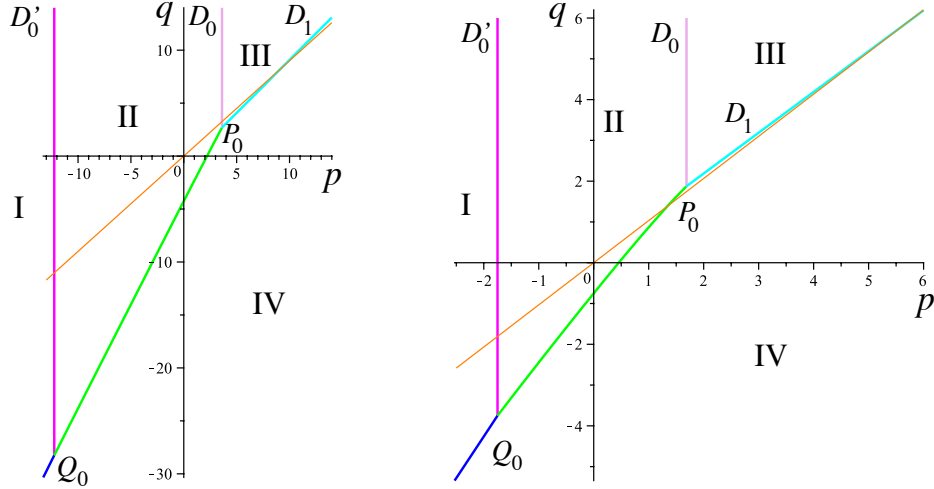


FIGURE 8. Phase diagram for the  $m$ -fold whole-plane  $\text{SLE}_\kappa$  in the  $(p, q_m)$ -plane, and trajectories (125) (coral color). Left: For  $m = +10$  and  $\kappa = 30$ , the line crosses successively domains I, II, III and IV. Right: For  $m = -30$  and  $\kappa = 2$ , the line crosses successively domains I, II, IV and III.

in the original  $(p, q)$  plane (Fig. 8). Let us consider the point  $P_0$  whose coordinates  $(p_0, q_0)$  are given by (100). The line  $OP_0$  has for slope  $\frac{q_0}{p_0} = \frac{2(8+\kappa)}{3(4+\kappa)}$ , a quantity that decreases from  $4/3$  to  $2/3$  as  $\kappa$  runs from  $0$  to  $\infty$  and takes the value  $1$  for  $\kappa = 4$ . As a consequence, for  $4 < \kappa$ , we have  $q_0/p_0 < 1$ , whereas for  $\kappa < 4$ ,  $1 < q_0/p_0$ .

In the first case, it is then possible to find  $m > 0$  such that  $\frac{q_0}{p_0} \leq 1 - \frac{1}{m} < 1$ . Observe that this inequality is precisely equivalent to (124) since  $4 < \kappa$ . The line (125) therefore first intersects the vertical line  $p = p_0$  above point  $P_0$ , and the line  $D_1$  of unit slope afterwards (Fig. 8). So the spectrum in this case has four phases,  $\beta_{\text{tip}}, \beta_0, \beta_{\text{lin}}$  and  $\beta_1$ , in this order from left to right.

In the second case, it is possible to find  $m < 0$  such that  $1 < 1 - \frac{1}{m} \leq \frac{q_0}{p_0}$ , an inequality again equivalent to (124), now in the case  $\kappa < 4$ . The line (125) thus crosses the line  $p = p_0$  at a point below point  $P_0$ . It follows that it first crosses the green parabola and then crosses the line  $D_1$ , after which the spectrum becomes linear (Fig. 8). So the spectrum again has four phases, but now in the order  $\beta_{\text{tip}}, \beta_0, \beta_1, \beta_{\text{lin}}$ .

The last example shows that the spectrum  $\beta_m(p, q; \kappa)$  (i.e.,  $\beta_1$  at  $(p, q_m)$ ) may appear even if the boundary of the SLE image domain is bounded. This indeed happens for  $m$  a negative integer: as seen in Section 5, the  $m$ -fold transform of the outer whole-plane SLE is then the conjugate by the inversion  $z \mapsto 1/z$  of the  $(-m)$ -fold transform of the inner whole-plane SLE, which gives rise to an univalent function map onto a domain with bounded boundary. In this case, the

appearance of the  $\beta_m$ , i.e.,  $\beta_1$  spectrum, is due to a high  $(-m)$ -fold branching at the origin for  $\kappa < 4$ .

## 7. A GEOMETRIC APPROACH

In this section, we develop an alternative approach for the study of the separatrix curves involved. Let us recall the four functions to compare,

$$\begin{aligned}\beta_1(p, q, \kappa) &= 3p - 2q - \frac{1}{2} - \frac{1}{2}\sqrt{1 + 2\kappa(p - q)}, \\ \beta_0(p, \kappa) &= -p + \frac{(4 + \kappa)^2}{4\kappa} - \frac{(4 + \kappa)}{4\kappa}\sqrt{(4 + \kappa)^2 - 8\kappa p}, \\ \beta_{\text{tip}}(p, \kappa) &= -p - 1 + \frac{1}{4}\left(4 + \kappa - \sqrt{(4 + \kappa)^2 - 8\kappa p}\right), \\ \beta_{\text{lin}}(p, \kappa) &= p - \frac{(4 + \kappa)^2}{16\kappa}.\end{aligned}$$

These functions are defined in the sector  $\mathcal{S}_\kappa$  such that

$$p < \frac{(4 + \kappa)^2}{8\kappa}, \quad 1 + 2\kappa(p - q) > 0.$$

Let us introduce a new system of coordinates,

$$x := \sqrt{(4 + \kappa)^2 - 8\kappa p}, \quad y := \sqrt{1 + 2\kappa(p - q)},$$

which defines a diffeomorphism from  $\mathcal{S}_\kappa$  onto the quarter plane  $\mathcal{A} = (\mathbb{R}^+)^2$ . The inverse diffeomorphism is given by

$$(126) \quad p = \frac{(4 + \kappa)^2 - x^2}{8\kappa}, \quad q = \frac{4 + (4 + \kappa)^2 - x^2 - 4y^2}{8\kappa}.$$

Note that this polynomial map is defined on the whole plane and maps each quarter plane bijectively onto  $\mathcal{S}_\kappa$ .

In the  $x, y$  variables, the above functions are

$$\begin{aligned}\beta_1 &= -\frac{x^2}{8\kappa} + \frac{y^2}{\kappa} - \frac{y}{2} + \frac{(4 + \kappa)^2}{8\kappa} - \frac{1}{2} - \frac{1}{\kappa}, \\ \beta_0 &= \frac{x^2}{8\kappa} - (4 + \kappa)\frac{x}{4\kappa} + \frac{(4 + \kappa)^2}{8\kappa}, \\ \beta_{\text{tip}} &= \frac{x^2}{8\kappa} - \frac{x}{4} - \frac{(4 + \kappa)^2}{8\kappa} + \frac{\kappa}{4}, \\ \beta_{\text{lin}} &= -\frac{x^2}{8\kappa} + \frac{(4 + \kappa)^2}{16\kappa}.\end{aligned}$$

We first study the set where  $\beta_1 = \beta_0$ . In the  $x, y$  variables, we have the nice factorization:

$$4\kappa(\beta_1 - \beta_0) = (2y + x - \kappa - 2)(2y - x + 2) =: \mathcal{R}(x, y) \mathcal{G}(x, y),$$

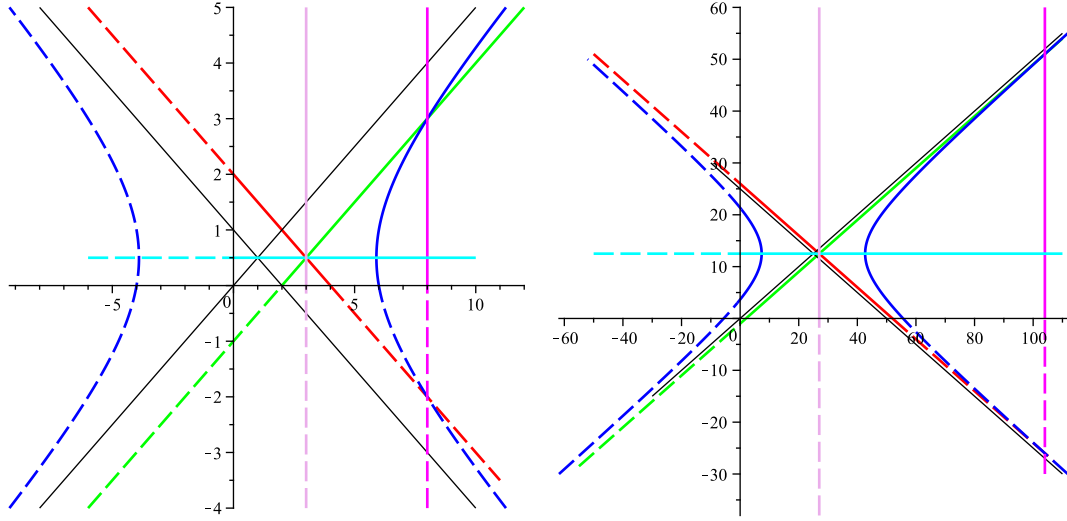


FIGURE 9. The separatrix curves in the  $(x, y)$ -plane for  $\kappa = 6$  and  $\kappa = 50$ . The dashed parts are lying outside of the first quarter  $\mathcal{A}$ .

and the set we are looking for is the intersection with  $\mathcal{A}$  of the union of the red,  $\mathcal{R}(x, y) = 0$ , and green,  $\mathcal{G}(x, y) = 0$ , straight lines (Fig. 9). Returning to the  $(p, q)$  variables, we get two portions of two parabolas  $\mathcal{R}$  and  $\mathcal{G}$ , that are both tangent to the two half-lines defining  $\mathcal{S}_\kappa$ . Using  $x$  as a parameter, we have the following parametric equations:

- For the red parabola  $\mathcal{R}$ ,

$$p = \frac{(4 + \kappa)^2 - x^2}{8\kappa}, \quad q = \frac{2(\kappa + 4) + (\kappa + 2)x - x^2}{4\kappa};$$

- For the green parabola  $\mathcal{G}$ ,

$$p = \frac{(4 + \kappa)^2 - x^2}{8\kappa}, \quad q = \frac{(4 + \kappa)^2 - 2x^2 + 4x}{8\kappa}.$$

Eliminating  $x$ , one easily gets the Cartesian equations of the corresponding sets:

- $\mathcal{R} : \left(\frac{\kappa + 2}{4\kappa}\right)^2 \left((4 + \kappa)^2 - 8\kappa p\right) = \left(q - 2p - \frac{(\kappa + 2)(\kappa + 4)}{4\kappa}\right)^2;$
- $\mathcal{G} : \frac{(4 + \kappa)^2 - 8\kappa p}{4\kappa^2} = \left(q - 2p + \frac{(4 + \kappa)^2}{8\kappa}\right)^2;$

they can also be respectively recast as Eqs. (25) and (118).

The set of points such that  $\beta_1 = \beta_{\text{lin}}$  is easier to compute, since

$$\beta_1 - \beta_{\text{lin}} = \frac{1}{\kappa} \left(y - \frac{\kappa}{4}\right)^2;$$

it is thus simply the line  $y = \kappa/4$ , i.e., in the  $(p, q)$ -plane, the straight line  $D_1$  such that  $q - p = \frac{(4+\kappa)(4-\kappa)}{32\kappa}$ .

In the same way as we found parabolae  $\mathcal{R}$  and  $\mathcal{G}$ , let us now discuss the set  $\mathcal{Q}$  of points  $(p, q)$  such that  $\beta_1(p, q) = \beta_{\text{tip}}(p)$ , i.e., the curve called the blue quartic in Section 6.3.4. In the  $x, y$  variables, this reads

$$(127) \quad 4\kappa(\beta_1 - \beta_{\text{tip}}) = 4\left(y - \frac{\kappa}{4}\right)^2 - \left(x - \frac{\kappa}{2}\right)^2 + 6(\kappa + 2) = 0,$$

and the set  $\mathcal{Q}$  is thus a hyperbola centered at  $(\kappa/2, \kappa/4)$ , whose pair of asymptotes is given by

$$(128) \quad (a) \ x - 2y = 0, \quad (b) \ x + 2y - \kappa = 0.$$

We easily deduce the parametric equations (in  $y$ ) of the set  $\mathcal{Q}$  in the  $(p, q)$ -plane:

$$(129) \quad p_{\pm} = \frac{(4 + \kappa)^2 - x_{\pm}^2}{8\kappa}, \quad q_{\pm} = p_{\pm} + \frac{1 - y^2}{2\kappa},$$

$$x_{\pm} := \frac{\kappa}{2} \pm \sqrt{4\left(y - \frac{\kappa}{4}\right)^2 + 6(\kappa + 2)}.$$

The Cartesian equation of the blue quartic  $\mathcal{Q}$  is then

$$\left((4 + \kappa)^2 - 8\kappa p\right) (1 + 2\kappa(p - q)) = \left(\frac{(\kappa + 4)^2}{4} + 1 - 2\kappa q - \left(4p - 2q - \frac{\kappa + 2}{4}\right)^2\right)^2,$$

an equation which can be shown to be equivalent to Eq. (120).

Using the (polynomial) map (126), we then get the desired set by taking the image of the intersection of hyperbola (127) with  $\mathcal{A}$ , i.e., a subset of an algebraic curve, here a quartic (Fig. 10). The (left) component of the quartic that will appear in the separatrices for the integral means spectrum is the image of the hyperbola's upper component, i.e., of the set parametrized by  $x_+$  in Eq. (129).

Note that the lower component has a relevant image in the  $(p, q)$ -plane only if it intersects  $\mathcal{A}$ , which happens iff  $x_-(\kappa/4) > 0$ , and is equivalent to  $\kappa > 12 + 8\sqrt{3}$ . (Fig. 10, right.) Then there exists a domain where  $\beta_1 \leq \beta_{\text{tip}} \leq \beta_0$ , thus with an irrelevant tip, and this component of the quartic has no bearing on the spectrum.

Let us conclude with the asymptotic study of the quartic. In  $(x, y)$ -coordinates, it is the hyperbola (127), with asymptotes (128). Near the first asymptote (a), this hyperbola is thus asymptotic to another one, with equation  $4y^2 - x^2 + 6(\kappa + 2) = 0$ . This becomes in the  $(p, q)$ -plane a straight line,  $q - 2p - (\kappa + 2)/8 = 0$ , which yields the linear asymptote in between the two components of the quartic (Fig. 11).

Similarly, near its second asymptote (b) in (128), the hyperbola is asymptotic to either one of the hyperbolae obtained by replacing, in the linear term  $x - 2y$  of Eq. (127), either  $x$  by  $\kappa - 2y$ , or  $2y$  by  $\kappa - x$ . In the  $(p, q)$  variables, these curves become two parabolae, whose equations have the generic form,  $\mathcal{P}(p, q) := (2p - q - 1/4)^2 - \kappa(p - q)/2 = c$ , for different values for  $c$ . Among this one-parameter

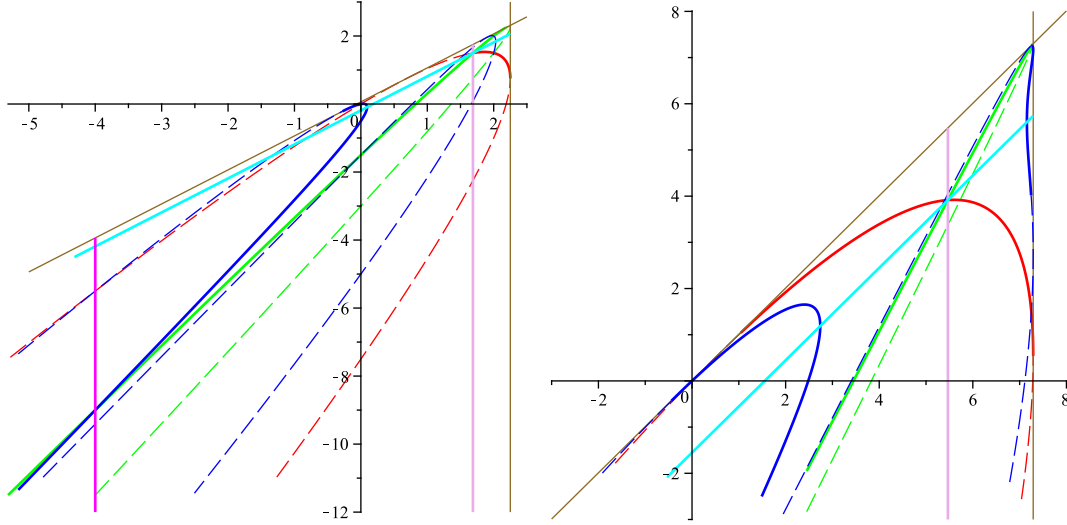


FIGURE 10. Image in the  $(p, q)$ -plane of Fig. 9 by the map (126), with corresponding solid/dashed parts. (Here  $\kappa = 8$  and  $\kappa = 50$ .)

family, there are a priori two distinguished ones, given by  $c = \lim_{p \rightarrow -\infty} \mathcal{P}(p, q)$ , for  $(p, q)$  belonging to the relevant branch in each component of the quartic. It happens that the limits are the same for both components, namely  $c = \frac{5}{8} + \frac{3}{16}\kappa$ . The blue quartic and its asymptotes are shown in Fig. 11.

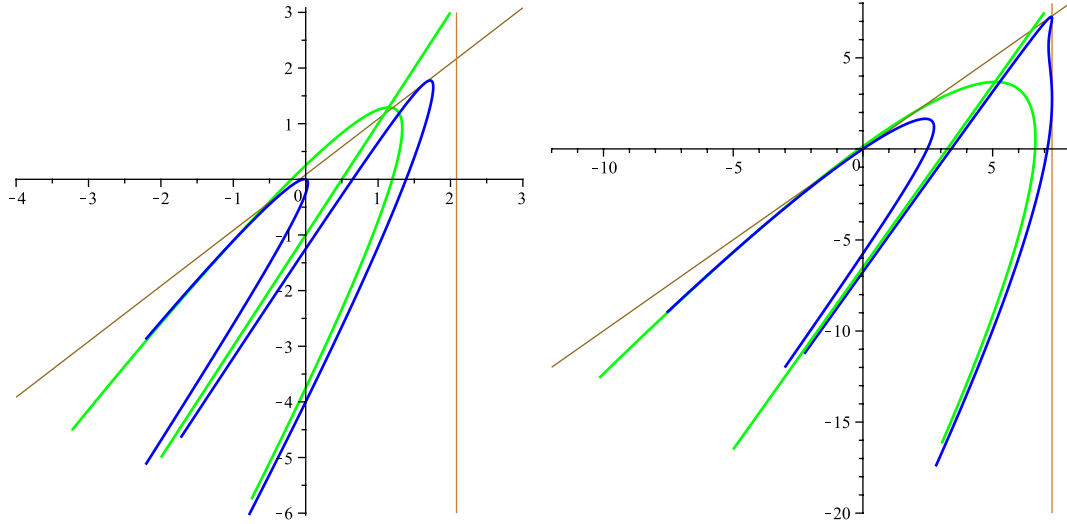


FIGURE 11. The quartic and its asymptotes in the  $(p, q)$ -plane for  $\kappa = 6$  and  $\kappa = 50$ .

## 8. UNIVERSAL SPECTRUM

It is worthwhile to compare the above results to universal ones. We aim at generalizing the universal spectrum for integral means of derivatives of univalent functions to the case of mixed integrals of the type:

$$\int_0^{2\pi} \frac{|f'(re^{i\theta})|^p}{|f(re^{i\theta})|^q} d\theta.$$

More precisely, for  $f$  injective and holomorphic in the unit disk, we define  $\beta_f(p, q)$  as being the smallest number such that

$$\int_0^{2\pi} \frac{|f'(re^{i\theta})|^p}{|f(re^{i\theta})|^q} d\theta \leq O(1-r)^{-\beta_f(p,q)-\varepsilon}, \forall \varepsilon > 0, r \rightarrow 1.$$

The *universal spectrum*  $B(p, q)$  is then defined as the supremum of  $\beta_f(p, q)$  over all holomorphic and injective  $f$ 's on the disk.

It should be first noticed that if one restricts oneself to bounded univalent functions, there will be no change with respect to the usual integral means spectrum, i.e., the denominator in the integrand (and thus  $q$ ) plays no role in this case. In the general case, we will mimic the Feng-McGregor approach [10].

**Theorem 8.1.** *Let  $f$  be holomorphic and injective in the unit disk. For  $p \in \mathbb{R}^+$ ,  $q \in \mathbb{R}$  such that  $q < \min\{2, \frac{5}{4}p - \frac{1}{2}\}$ , there exists a constant  $C > 0$  such that*

$$(130) \quad \int_0^{2\pi} \frac{|f'(re^{i\theta})|^p}{|f(re^{i\theta})|^q} d\theta \leq \frac{C}{(1-r)^{3p-2q-1}}.$$

The universal spectrum is therefore finite and such that  $B(p, q) \leq 3p - 2q - 1$ , at least in the domain  $\mathcal{D}_0 := \{0 \leq p, q < \min\{2, \frac{5}{4}p - \frac{1}{2}\}\}$  of Theorem 8.1. In that domain, the Koebe function,  $\mathcal{K}(z) = z(1+z)^{-2}$ , saturates the bound, therefore  $B(p, q) = 3p - 2q - 1 > 0$  for  $(p, q) \in \mathcal{D}_0$ .

In order to make the proof lighter, we will neither write the variables in the functions involved, which are of the form  $re^{i\theta}$  with  $r$  fixed, nor the angular integration interval, which is meant to be  $[0, 2\pi]$ .

*Proof.* Let  $a, b$  be two reals, to be fixed later, such that  $a - b = 1$ . Let us first consider the case  $p < 2$ , for which Hölder's inequality gives

$$(131) \quad \int \frac{|f'|^p}{|f|^q} = \int \frac{|f'|^p}{|f|^{aq}} |f|^{bq} \leq \left( \int \frac{|f'|^2}{|f|^{2aq/p}} \right)^{p/2} \left( \int |f|^{2bq/(2-p)} \right)^{(2-p)/2}.$$

In order to estimate the first integral on the right-hand side, we invoke Hardy's inequality [25]: For any  $p' > 0$ , there exists a constant  $C' > 0$  such that for any function  $f$  which is holomorphic and injective in the unit disk,

$$\int |f'|^2 |f|^{p'-2} \leq \frac{C'}{(1-r)^{2p'+1}}.$$



For the rightmost integral in (131), we use the Prawitz inequality [25]: For any  $p'' > 1/2$ , there exists a constant  $C'' > 0$  such that for any function  $f$  holomorphic and injective in the unit disk,

$$\int |f|^{p''} \leq \frac{C''}{(1-r)^{2p''-1}}.$$

We then take  $p' := 2 - \frac{2aq}{p}$ ,  $p'' := \frac{2bq}{2-p}$ , and assume that  $p' > 0$  and  $p'' > 1/2$ ; we may then use the two inequalities above and get from (131)

$$(132) \quad \int \frac{|f'|^p}{|f|^q} \leq \frac{C}{(1-r)^{3p-2q-1}},$$

for some  $C > 0$  and any  $f$  as above. For this, we need to find  $a, b \in \mathbb{R}$  such that

$$a - b = 1, \quad p' > 0, \quad p'' > 1/2.$$

The first inequality is equivalent to  $p > aq$ , and the second one gives  $aq > q + \frac{2-p}{4}$ . We thus find that the universal bound (132) holds for

$$q + \frac{1}{2} < \frac{5}{4}p.$$

Recall then the original condition of validity,  $p < 2$ , which implies that  $q < 2$ . The theorem being already proved for  $p < 2$ , we may now assume that  $p \geq 2$ . Let then  $p'$  be such that  $\frac{4}{5}q + \frac{2}{5} < p' < 2 \leq p$ . We now invoke Koebe distortion theorem:

$$\forall z \in \mathbb{D}, \quad |f'(z)| \leq 2 \frac{|f'(0)|}{(1-|z|)^3},$$

from which follows, by writing  $|f'|^p = |f'|^{p'} |f'|^{p-p'}$  and by using (130) for the couple  $(p', q)$ , that for some  $C > 0$ ,

$$(133) \quad \int \frac{|f'|^p}{|f|^q} \leq \frac{C}{(1-r)^{3p'-2q-1+3(p-p')}} = \frac{C}{(1-r)^{3p-2q-1}}.$$

□

Guided by the results obtained above for the generalized integral means spectrum of whole-plane SLE, we will now state a conjecture concerning the universal generalized spectrum. As we shall see, its structure turns out to be very similar, each of the SLE four spectra having its own analogue in the universal case.

Let us first recall that the universal spectrum for **bounded** holomorphic and injective functions,  $B(p)$ , is known to be equal to  $p - 1$  for  $p \geq 2$ , and equal to  $-p - 1$  below a certain threshold  $p^\dagger \leq -2$ . For  $p \in [p^\dagger, 2]$ , it is equal to an unknown function,  $B_0(p)$ . Two famous conjectures are that by Brennan, stating that  $B_0(-2) = 1$  and implying that  $p^\dagger = -2$ , and the broader conjecture by Kraetzer stating that  $B_0(p) = p^2/4$  (see Ref. [25] and references therein).

For **unbounded** functions, a classical result by Makarov [23] states that the universal spectrum is simply given by

$$(134) \quad \max\{B(p), 3p - 1\},$$

the second term corresponding to the extremal case of the Koebe function.

Now, in the case of generalized spectra, the universal analogue of the SLE generalized spectrum  $\beta_1(p, q; \kappa)$  is naturally the spectrum that we have just obtained in Theorem 8.1, and that corresponds to the Koebe limit of Section 6.4.3,

$$(135) \quad B_1(p, q) := 3p - 2q - 1.$$

The analogue of the SLE bulk spectrum,  $\beta_0(p)$ , is then naturally given by the function  $B_0(p)$  of the bounded universal spectrum above, while the two remaining SLE spectrum functions,  $\beta_{\text{tip}}(p)$  and  $\beta_{\text{lin}}(p)$ , have respectively for universal analogues,  $B_{\text{tip}}(p) := -p - 1$  for  $p \leq p^\dagger$ , and  $B_{\text{lin}}(p) := p - 1$  for  $p \geq 2$ .

We then proceed as for SLE, looking for the sets of points in the  $(p, q)$  plane such that  $B_1(p, q) = B_{\text{tip}}(p)$ ,  $B_1(p, q) = B_0(p)$ ,  $B_1(p, q) = B_{\text{lin}}(p)$ . They turn out to be, in the same order,

- the line  $q = 2p$  for  $p \leq p^\dagger$ ,
- the curve  $2q = 3p - 1 - B_0(p)$  for  $p \in [p^\dagger, 2]$ ,
- the line  $p = q$  for  $p \geq 2$ .

Note that if Brennan's conjecture holds,  $p^\dagger = -2$ , and it is equivalent to the fact that the separatrix curve,  $2q = 3p - 1 - B_0(p)$ , the vertical line,  $p = -2$ , and the separatrix,  $q = 2p$ , all meet at point  $(-2, -4)$ . If Kratzer's conjecture also holds, the first curve becomes the segment of parabola  $2q = 3p - 1 - p^2/4$ , with  $p \in [-2, 2]$ .

In complete analogy with the SLE case (see Fig. 5), we thus obtain a prediction for the universal spectrum  $B(p, q)$ , with a partition of the plane into four zones corresponding to the four spectra introduced above, as illustrated in Fig. 12. Observe that the above picture contains, for  $q = 0$ , the universal spectrum for all univalent functions, as well as, along the line  $q = 2p$ , the spectrum of bounded univalent ones. For  $p \leq p^\dagger$  (possibly  $(-2)$ ), the latter line also appears as a *separatrix* of the (conjectured) universal spectrum. A small departure from it triggers a phase transition in the spectrum, which is thus *unstable* along the bounded functions line.

*Remark 8.2.* As work done with Kari Astala shows [1], it is actually possible to extend Makarov's approach [23] to the universal generalized spectrum  $B(p, q)$ , and to generalize the result (134) into

$$B(p, q) = \max\{B(p), 3p - 2q - 1\},$$

therefore entirely confirming the conclusions drawn above for the universal generalized spectrum, the unknown remaining the position of  $p^\dagger$  and the form of  $B_0(p)$  in the standard universal spectrum.

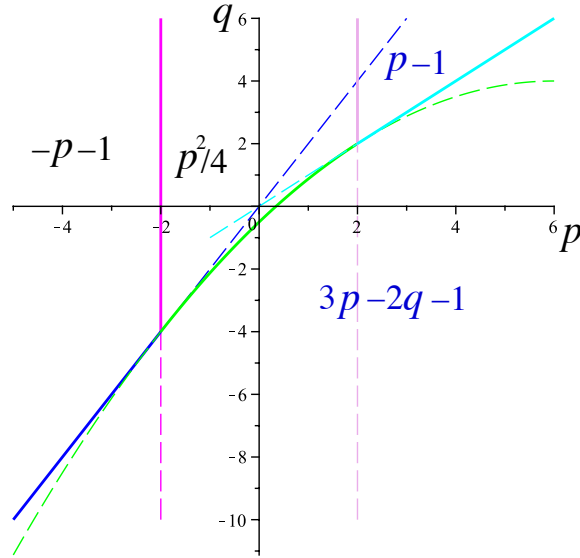


FIGURE 12. The four functions giving the universal generalized spectrum (assuming here the validity of Kraetzer’s conjecture).

## REFERENCES

- [1] K. Astala, B. Duplantier, and M. Zinsmeister, 2015. Unpublished.
- [2] D. Beliaev, B. Duplantier, and M. Zinsmeister. Integral Means Spectrum of Whole-Plane SLE, 2015. In preparation.
- [3] D. Beliaev and S. Smirnov. Harmonic Measure and SLE. *Commun. Math. Phys.*, 290:577–595, 2009.
- [4] L. Bieberbach. Über die Koeffizienten derjenigen Potenzreihen, welche eine schlichte Abbildung des Einheitskreises vermitteln. *S-B. Preuss. Akad. Wiss.*, 1:940–955, 1916.
- [5] L. de Branges. A proof of the Bieberbach conjecture. *Acta Math.*, 154:137–152, 1985.
- [6] B. Duplantier. Conformally Invariant Fractals and Potential Theory. *Phys. Rev. Lett.*, 84:1363–1367, 2000.
- [7] B. Duplantier. Conformal fractal geometry & boundary quantum gravity. In M. L. Lapidus and M. van Frankenhuysen, editors, *Fractal geometry and applications: a jubilee of Benoît Mandelbrot, Part 2*, volume 72 of *Proc. Sympos. Pure Math.*, pages 365–482. Amer. Math. Soc., Providence, RI, 2004.
- [8] B. Duplantier, Nguyen Thi Phuong Chi, Nguyen Thi Thuy Nga, and M. Zinsmeister. Coefficient estimates for whole-plane SLE processes. *Hal-00609774*, 20 Jul. 2011.
- [9] Bertrand Duplantier, Chi Nguyen, Nga Nguyen, and Michel Zinsmeister. The Coefficient Problem and Multifractality of Whole-Plane SLE and LLE. *Ann. Henri Poincaré*, 16(6):1311–1395, 2014. ArXiv:1211.2451v2[math-ph].
- [10] J. Feng and T. H. MacGregor. Estimates on the integral means of the derivatives of univalent functions. *J. Anal. Math.*, 29:203–231, 1976.
- [11] John B. Garnett and Donald E. Marshall. *Harmonic Measure*. Cambridge University Press, 2005.
- [12] H. Grunsky. Koeffizienten Bedingungen für schlicht abbildende meromorphe Funktionen. *Math. Z.*, 45:29–61, 1939.

- [13] A. Kemppainen. Stationarity of SLE. *J. Stat. Phys.*, 139:108–121, 2010.
- [14] K. Kytölä and A. Kemppainen. SLE local martingales, reversibility and duality. *J. Phys. A: Math. Gen.*, 39:L657–L666, 2006.
- [15] G. F. Lawler, O. Schramm, and W. Werner. Values of Brownian intersection exponents. II. Plane exponents. *Acta Math.*, 187(2):275–308, 2001.
- [16] Thanh Binh Le. Around Milin’s conjecture and SLE maps, 2010. Mémoire de M2, Université d’Orléans.
- [17] N. A. Lebedev and I. M. Milin. On the coefficients of certain classes of univalent functions. *Mat. Sb.*, 28:359–400, 1951. (In Russian).
- [18] I. Loutsenko. SLE $_{\kappa}$ : correlation functions in the coefficient problem. *J. Phys. A Math. Gen.*, 45(26):265001, 2012.
- [19] I. Loutsenko and O. Yermolayeva. On exact multi-fractal spectrum of the whole-plane SLE. *ArXiv:1203.2756*, 2012.
- [20] I. Loutsenko and O. Yermolayeva. Average harmonic spectrum of the whole-plane SLE. *J. Stat. Mech.*, page P04007, 2013.
- [21] I. Loutsenko and O. Yermolayeva. On Harmonic Measure of the Whole Plane Lévy-Loewner Evolution. *ArXiv:1301.6508*, 2013.
- [22] K. Löwner. Untersuchungen über schlichte konforme Abbildungen des Einheitskreises. *Math. Annalen*, 89:103–121, 1923.
- [23] N. G. Makarov. Fine structure of harmonic measure. *Rossiiskaya Akademiya Nauk. Algebra i Analiz*, 10:1–62, 1998. English translation in *St. Petersburg Math. J.* 10: 217-268 (1999).
- [24] I. M. Milin. Estimation of coefficients of univalent functions. *Dokl. Akad. Nauk SSSR*, 160:196–198, 1965.
- [25] Ch. Pommerenke. *Boundary Behaviour of Conformal Maps*. Grundlehren der mathematischen Wissenschaften, Vol. 299. Springer, Berlin, 1992.
- [26] M. S. Robertson. On the theory of univalent functions. *Ann. of Math.*, 37:374–408, 1936.
- [27] S. Rohde and O. Schramm. Basic Properties of SLE. *Ann. of Math.*, 161:883–924, 2005.
- [28] O. Schramm. Scaling limits of loop-erased random walks and uniform spanning trees. *Israel J. Math.*, 118:221–288, 2000.

<sup>(1)</sup>INSTITUT DE PHYSIQUE THÉORIQUE, CEA/SACLAY, F-91191 GIF-SUR- YVETTE CEDEX, FRANCE

*E-mail address:* `bertrand.duplantier@cea.fr`

<sup>(2)</sup>MAPMO, UNIVERSITÉ D’ORLÉANS, BÂTIMENT DE MATHÉMATIQUES, RUE DE CHARTRES B.P.6759-F-45067 ORLÉANS CEDEX 2, FRANCE

*E-mail address:* `hoxhieu@gmail.com`

*E-mail address:* `mr.lethanhbinh@gmail.com`

*E-mail address:* `zins@univ-orleans.fr`